

Low spin spectroscopy of neutron-rich $^{43,44,45}\text{Cl}$ via β^- and βn decay

Vandana Tripathi^{1a}, Soumik Bhattacharya¹, E. Rubino^{1,9}, C. Benetti^{1,3},
 J. F. Perello¹, S. L. Tabor¹, S. N. Liddick^{2,3,4}, P. C. Bender⁵, M. P. Carpenter⁶,
 J. J. Carroll⁷, A. Chester^{2,3}, C. J. Chiara⁷, K. Childers^{2,4}, B. R. Clark⁸,
 B. P. Crider⁸, J. T. Harke⁹, R. Jain^{3,10}, B. Longfellow^{2,10,9}, S. Luitel⁸,
 M. Mogannam^{3,4}, T. H. Ogunbeku⁸, A. L. Richard^{2,9}, S. Saha⁵, N. Shimizu¹¹,
 O. A. Shehu⁸, Y. Utsuno^{12,13}, R. Unz⁸, Y. Xiao⁸, S. Yoshida¹⁴, and Yiyi Zhu⁵

¹*Department of Physics, Florida State University, Tallahassee, Florida 32306, USA*

²*National Superconducting Cyclotron Laboratory,*

Michigan State University, East Lansing, MI 48824, USA

³*Facility for Rare Isotope Beams, Michigan State University,
 East Lansing, Michigan 48824, USA*

⁴*Department of Chemistry, Michigan State University,
 East Lansing, Michigan 48824, USA*

⁵*Department of Physics, University of Massachusetts
 Lowell, Lowell, Massachusetts 01854, USA*

⁶*Argonne National Laboratory, Argonne, Illinois 60439, USA*

⁷*U.S. Army Combat Capabilities Development Command
 Army Research Laboratory, Adelphi, Maryland 20783 USA*

⁸*Department of Physics and Astronomy,
 Mississippi State University, Mississippi State, MS 39762, USA*

⁹*Lawrence Livermore National Laboratory, Livermore, California 94550, USA*

¹⁰*Department of Physics and Astronomy,
 Michigan State University, East Lansing, Michigan 48824, USA*

¹¹*Center for Computational Sciences,
 University of Tsukuba, Tennodai, Tsukuba 305-8577, Japan*

¹²*Advanced Science Research Center,
 Japan Atomic Energy Agency, Tokai, Ibaraki 319-1195, Japan*

^a Corresponding author: vtripath@fsu.edu

¹³*Center for Nuclear Study, University of Tokyo,
Hongo, Bunkyo-ku, Tokyo 113-0033, Japan and*

¹⁴*Liberal and General Education Center,
Institute for Promotion of Higher Academic Education,
Utsunomiya University, Mine, Utsunomiya, Tochigi 321-8505, Japan*

(Dated: November 21, 2023)

Abstract

β^- decay of neutron-rich isotopes $^{43,45}\text{S}$, studied at the National Superconducting Cyclotron Laboratory is reported here. β -delayed γ transitions were detected by an array of 16 clover detectors surrounding the Beta Counting Station which consists of a 40x40 Double Sided Silicon Strip Detector followed by a Single Sided Silicon Strip Detector. β -decay half-lives have been extracted for $^{43,45}\text{S}$ by correlating implants and decays in the pixelated implant detector with further coincidence with γ transitions in the daughter nucleus. The level structure of $^{43,45}\text{Cl}$ is expanded by the addition of 20 new γ transitions in ^{43}Cl and 8 in ^{45}Cl with the observation of core excited negative-parity states for the first time. For ^{45}S decay, a large fraction of the β decay strength goes to delayed neutron emission populating states in ^{44}Cl which are also presented. Comparison of experimental observations is made to detailed shell-model calculations using the *SDPFSDG – MU* interaction to highlight the role of the diminished $N = 28$ neutron shell gap and the near degeneracy of the proton $s_{1/2}$ and $d_{3/2}$ orbitals on the structure of the neutron-rich Cl isotopes. The current work also provides further support to a ground state spin-parity assignment of $3/2^+$ in ^{45}Cl .

I. INTRODUCTION

^{48}Ca is a doubly magic nucleus, characterized by a spherical shape which is stabilized by the $Z = 20$ and $N = 28$ shell closures. However, down the isotonic chain, ^{44}S displays clear evidence of shape mixing or co-existence by the presence of an isomeric low-lying 0_2^+ state [1]. For ^{46}Ar , an isotope between ^{48}Ca and ^{44}S the situation seems more nuanced. The systematics of 2_1^+ energies in the Ar isotopic chain indicate a pronounced shell gap but there remains the question that shell model calculations, irrespective of the interaction used, predict a high $B(E2)$ value in contradiction with the high-lying 2^+ state [2, 3] in ^{46}Ar . Further, based on recent mass measurements of $^{46-48}\text{Ar}$ the extracted one- and two-neutron shell gaps indicate the presence of a persistent, but reduced empirical shell gap in ^{46}Ar compared to the doubly magic ^{48}Ca [4]. The occurrence of spherical or deformed shapes in nuclei is intimately related to the nucleonic structure; for the exotic $N = 28$ isotones, deformation sets in due to the melting of the $N = 28$ shell gap along with the closing of the $Z = 16$ spherical gap. Hence the understanding of the single particle structure in the vicinity of ^{46}Ar is very important which appears to be the transition between doubly magic ^{48}Ca and the more collective ^{44}S .

Spectroscopy of odd-odd and odd-even nuclei can provide valuable information to test the single particle structure and benchmark calculations. Neutron-rich Cl isotopes with proton holes in the sd shell approaching the $N = 28$ magic number can shed light on the single particle structure in this interesting region of the chart of nuclides. However spectroscopic information for $A > 40$ isotopes of Cl is rather limited due to the difficulty in producing those for investigation [5–7]. The most exhaustive information comes from in-beam γ -ray spectroscopy following fragmentation performed at NSCL for $^{43-46}\text{Cl}$ [7] where γ - γ coincidences were used to generate experimental level schemes up to ≈ 2 MeV for ^{43}Cl , ^{45}Cl , and ^{46}Cl , although no firm spin assignments could be made from that measurement. Very recently the first γ -ray spectroscopy of $^{47,49}\text{Cl}$ was performed at the Radioactive Isotope Beam Factory (RIBF) with ^{50}Ar projectiles impinging on a liquid hydrogen target to produce the exotic isotopes [8]. Through the one-proton knockout reaction, a spin-parity, $J^\pi = 3/2^+$ was proposed for the ground state of ^{49}Cl .

For the odd-A Cl isotopes with $N > 20$ filling of neutrons in the $f_{7/2}$ orbital may cause inversion between the $\pi s_{1/2}$ and $\pi d_{3/2}$ orbitals. The strong monopole proton-neutron inter-

action between the $\pi d_{3/2}$ and $\nu f_{7/2}$ orbits acts attractively on the $\pi d_{3/2}$ orbital, lowering its energy with respect to the $\pi s_{1/2}$ orbital when the $\nu f_{7/2}$ orbital is being filled for the $N \approx 28$ nuclei. It is anticipated that there will be a reversion back to the normal ordering for larger neutron excess (neutrons filling the $\nu p_{3/2}$ orbit) where the neutron-proton interaction between the $\pi s_{1/2}$ and $\nu p_{3/2}$ orbits comes into play. These changes in the single particle ordering can impact properties of ground and excited states of nuclei. For nearby odd-A K isotopes ($Z = 19$) the ground-state spin inversion of $3/2^+$ to $1/2^+$ is observed for $A = 47 - 49$ [6, 9]. In the case of Cl isotopes, direct spin measurements have not been performed for the neutron rich isotopes, however a picture similar to K can be drawn from other experimental information.

In ^{41}Cl the ground state is favored to be $1/2^+$ [10–12]. This is based on an analogy with the lighter isotopes where the yrast $5/2_1^+$ level decays exclusively to the $3/2^+$ and not to the $1/2^+$ level. The β -decay of ^{41}S to ^{41}Cl [13] also supports a $1/2^+$ assignment, however $3/2^+$ cannot be ruled out completely based on these observations. For ^{43}Cl strong evidence in favor of an inverted ground state of $1/2^+$ comes from the in-beam γ spectroscopy following fragmentation where the angular distribution of the 330-keV transition which connects the ground state to the first excited state was measured [5]. The anisotropy of the 330-keV transition rules out that it is a decay from a $1/2^+$ state making the ground state spin to be $1/2^+$ instead. However a reverse conclusion is drawn from the β -decay study of ^{43}Cl to ^{43}Ar [14]. That is based on the observed branching to the ground state of 28(10)% with 5.81 as a lower limit of the $\log ft$. The ground state of ^{43}Ar being $5/2^-$, this $\log ft$ could correspond to a First Forbidden (FF) β transition but only if ^{43}Cl ground state is $3/2^+$. This is a much weaker argument in favor of the $3/2^+$ assignment as extracting ground state branching has its limitations. The assignment of a $3/2^+$ to the ground state of ^{45}Cl has more support than $^{41,43}\text{Cl}$. In Ref. [7], the life time of the lowest 130-keV transition was measured to be 470(60) ps yielding a $B(M1)_{exp} = 0.055\mu_N^2$ which is better reproduced by shell model calculation in that work for a $3/2^+$ ground state. Additionally in the one proton knockout from ^{45}Cl to ^{44}S by Riley et al, [15], the population of the 4_1^+ in ^{44}S provides a strong argument for a $3/2^+$ ground state in ^{45}Cl . A $1/2^+$ ground state for ^{45}Cl would lead to an unmeasurably small cross section for the 4_1^+ state based on shell model calculation. In our own recent study of the β^- -decay of ^{45}Cl to ^{45}S , a $3/2^+$ assignment was favored over $1/2^+$ based on the strong population of the $5/2^+$ state in the daughter [16]. Moving to

more exotic isotopes, a $J^\pi = 3/2^+$ was proposed for the ground state of ^{49}Cl in the RIBF experiment [8] as mentioned before, though the ground-state for ^{47}Cl is not yet confirmed, but likely to be $3/2^+$.

In the odd-A Cl isotopes, the negative-parity states arise from the excitation of the unpaired proton or one of the sd neutrons to the fp shell. In the stable ^{37}Cl with $N = 20$ a sequence of $7/2^-$ - $9/2^-$ - $11/2^-$ - $13/2^-$ states is observed with the $7/2^-_1$ state at 3.1 MeV [17, 18]. For ^{39}Cl the negative-parity states occur at about half the excitation energy with a sequence of $5/2^-$ - $7/2^-$ - $9/2^-$ - $11/2^-$ states starting at 1697 keV [19]. The information for more exotic ^{41}Cl is sparse with only two tentative negative-parity states proposed at 1475 keV ($5/2^-$, $7/2^-$) and 2718 keV ($5/2^-$, $7/2^-$) [19] with none known for $^{43,45}\text{Cl}$.

The current work is an effort to enhance the spectroscopic information on exotic Cl isotopes and we have studied β^- decay of $^{43,45}\text{S}$ to access excited states in the daughters $^{43,44,45}\text{Cl}$. The β -decay half-life of ^{43}S has been reported earlier [13, 20, 21] with an evaluated value of 265(15) ms [22], however none followed the γ transitions in the daughter nucleus. Similarly the literature value for ^{45}S half-life is 68(2) ms [20, 23] from implant- β^- correlations performed at GANIL. The current work, to our knowledge, will be the first to report on β -delayed γ transitions in the daughter nuclei $^{43,44,45}\text{Cl}$ to complement the limited information from in-beam γ spectroscopy. For the $N = 26$ ^{43}Cl 20 new transitions have been identified while 8 new ones have been added for the $N = 28$ ^{45}Cl . β^- decay from the $N = 27, 29$ isotopes of S which have negative-parity ground states will feed negative-parity intruder states via Gamow-Teller (GT) β transitions, reported here for the first time.

The experimental results are interpreted within configuration interaction Shell Model (SM) calculations using the $SDPFSDG - MU$ interaction within a model space of the sd - pf - sdg shells [24, 25] with some truncation on $1p1h$ excitations across either the $Z = N = 20$ or $N = 40$ shell gaps. Protons are allowed to move only from the sd to the pf shell while one neutron excitations from sd to pf and pf to sdg (for $N > 20$) shells are explicitly taken into account. The valence space contains the sd orbitals for protons and the fp orbitals for neutrons, with a ^{16}O inert core. The interactions used for the sd shell, pf shell, and the cross shell are respectively, USD, GXPF1B, and a variant of the V_{MU} that was employed for the $SDPF - MU$ interaction [24]. The calculations predict very close-by $3/2^+$ and $1/2^+$ states with one being the ground state for odd-A Cl isotopes. Closer to stability $3/2^+$ is the preferred ground state which switches to $1/2^+$ for ^{41}Cl due to the near degeneracy of $s_{1/2}$

and $d_{3/2}$ proton orbitals together with enhanced collectivity.

II. EXPERIMENTAL SETUP

The experiment was carried out at the National Superconducting Cyclotron Laboratory (NSCL) [26] at Michigan State University where a ^{48}Ca primary beam was fragmented to produce several exotic isotopes of P, S and Cl with neutron number around 28. Some interesting results from this data can be found in Refs. [16, 27] and further details of the setup can also be found there. The primary beam was accelerated to 140 MeV/u and then fragmented on a thick ^9Be target at the target position of the fragment separator, the A1900 [28], and further dispersed through a wedge-shaped Al degrader positioned at the intermediate dispersive image of the A1900. ^{43}S and ^{45}S were produced using two different settings of the A1900 with 1% and 2% momentum acceptance respectively.

In the two cases ^{43}S and ^{45}S isotopes (along with others) were implanted in a pixelated (40 strips x 40 strips) Double-Sided Silicon Strip Detector (DSSD), which is part of the Beta Counting Setup (BCS). An Al degrader placed upstream ensured that the implants stopped roughly at the middle of the 1mm thick DSSD. The DSSD was followed by a Single-Sided Silicon Strip Detector (SSSD) which served as a veto detector for light ions passing through. A low implant rate of about 150/s ensures clean correlations between the implants and decay events. Two Si PIN detectors placed upstream of the DSSD provided the energy loss and time of flight information which, along with the scintillator at the intermediate dispersive image of the A1900 were used for particle identification of the incoming implants at the BCS. The DSSD and SSSD stack was surrounded by 16 Clover detectors to record the β -delayed γ rays with a total singles efficiency of about 5% at 1 MeV after addback. Energy and efficiency calibration was performed using standard γ sources up to 3.5 MeV. The data were collected event by event using the NSCL digital data acquisition system [29]. Each channel provided its own time-stamp signal, which allowed coincidences and correlations to be built in the analysis offline.

γ transitions coincident with β correlated implants for ^{43}S and ^{45}S decays are shown in the top and bottom panel of Figure 1 respectively. For both a correlation window roughly equal to the half-life of parent was chosen to showcase the β -delayed γ transitions in the daughter. Random correlations were avoided by subtracting γ transitions associated with

a very long correlation window. Most of the strong transitions in the daughter nucleus are clearly observed and later the γ - γ coincidences will be discussed which allowed us to build the level schemes.

III. EXPERIMENTAL RESULTS

A. ^{43}S (Z=16; N=27) β^- decay

In a typical continuous beam β -decay experiment with fast fragmentation beams the half-life extraction requires event by event time correlation between β particles and the precursor implants. Such time and spatial correlation was followed in the current analysis to generate decay curves. Figure 2 (a) shows the decay curve for the ^{43}S implants for a correlation time window of 2 seconds. The figure also shows the fit following Bateman equations yielding a value of 256(5) ms for the half-life of ^{43}S similar to the evaluated value of 265(15) ms from prior studies [22]. In the fit the contribution of $\beta 1n$ daughter *i.e.* the P_n value was taken to be 40(10) % [21, 23]. For further confirmation, the half-life was also obtained by fitting the time distribution of the γ -ray transitions at 329- and 879 keV in the $\beta 0n$ daughter as shown in Figure 2 (b). An exponential fit with a constant background yields a half-life of 250.2(25) ms. According to SM calculations discussed earlier using the $SDPFSDG - MU$ interaction [30], predictions for the ^{43}S half-life with a $3/2^-$ ground state are 336 ms when including First Forbidden (FF) β transitions and 360 ms when considering only GT transitions. Both these values are longer than the measured value, possibly correlated to the prediction of a low P_n value of only 8% by the shell model calculations [30].

The level-scheme of ^{43}Cl derived from the current delayed γ -ray spectroscopy is shown in Figure 3. The energy levels up to 1927 keV with 6 γ transitions were known from the prior studies [5, 7, 10]. We have been able to extend the level-scheme to 5612 keV with 20 newly identified γ -ray transitions, shown in red. Placement of all the newly observed γ -ray transitions were confirmed with γ - γ coincidences. Figure 4 shows the γ -ray peaks in coincidence with the previously-known ground-state transitions at 329 keV (a,b) and 879 keV (c). The 879 keV level with a direct decay to the ground state was only tentatively placed in Ref. [7]. Prior to that, the 881 keV (879 in this work) was proposed to depopulate a 1830-keV level feeding into the 941 keV state [5]. However being the second strongest

transition and showing no coincidence with the 329-keV transition (Figure 4), we propose that the 879-keV transition comes from an excited state at the same energy ratifying the tentative placement in Ref. [7]. The decay of the 2022 keV level to both the 879-keV and 329-keV states, among others, confirms further the placement of the 879-keV transition. The placement of the 1509-keV transition from Ref. [5] (1507 keV in this work) is also confirmed by its coincidence with the 329-keV transition. The coincidence of the highest energy γ peaks 4744 and 5280 keV with the 329 keV transition are shown in panels (d) and (e) in the same figure. Table I gives the details of all the γ transitions where the absolute intensity was calculated using the measured peak area, γ detection efficiency and the number of implants obtained from the fit to the decay curve. The $\log ft$ values for the excited states above the 1927 keV level which we believe are directly populated in the β decay via GT transitions were calculated using the NNDC $\log ft$ calculator [31] making use of the measured $T_{1/2}$ and absolute β branching and the known Q_{β^-} value [32].

B. ^{45}S ($Z=16$; $N=29$) β^- decay

The decay curves for ^{45}S decay with and without coincidence with γ transitions in the daughter nucleus are shown in Figure 5. The decay curve from the implant- β correlations was fitted similar to ^{43}S and a half-life of 69(1) ms was extracted in excellent agreement with the previous measurement from Ref. [20]. Figure 5 (b) shows the time distribution of the 132 keV lowest transition in ^{45}Cl and an exponential fit yields a half-life of 74(5) ms, the higher error bar is due to lower statistics. Contrary to the case of ^{43}Cl the calculated half-life from the SM calculation after including both the GT and FF transitions at 70.7 ms agrees well with the measured value. Excluding the FF transitions predicts 78.5 ms, slightly longer than the measured value. This is under the assumption that the ground state of ^{45}S is $3/2^-$ which is expected from the filling of the $\nu p_{3/2}$ orbital for the $N = 29$ isotope.

The β -delayed γ transitions were studied to construct the level scheme of daughter ^{45}Cl . The known γ transitions at 132-, 633-, 765-, 929-, and 1619 keV [7] were clearly observed and are shown in black in Figure 6. The 132-, 633-, 765-, and the 929 keV transitions were also observed in the β -delayed one-neutron emission from ^{46}S published earlier by us [27]. Accurate energy values for these transitions are determined in this work as detailed in Table II. Whenever possible γ - γ coincidences were explored to place the observed transitions, and

some of the coincidences are shown in Figure 7. A 1081 keV transition is seen in clear coincidence with the 1619 keV decay and hence proposed to feed that level. In Ref. [7] where states in ^{45}Cl were investigated following fragmentation, a 1061(9) keV transition was placed above the 1619 keV transition, however we do not observe that transition. Instead our observation is of the 1081 keV γ ray. As the new transition is outside of error bar on the 1061 keV transition we have shown it as red in Figure 6 though the two could likely be the same transition with the β decay spectrum giving a determination of energy closer to the true value.

Coincidences are also observed between the 1462 keV and 929 keV transitions and hence 1462 is placed feeding the 929 keV level in departure from Ref. [7] where a transition of the same energy was considered a ground state transition. In the same work a 1950 keV transition was observed (tentative) but not placed in the level scheme. Based on coincidences observed between the 929 keV and 1020 keV transitions as seen in Figure 7 (a) we determined a level at 1949 keV. The direct decay from the level is also present but is partly obscured by a long lived activity line at 1945 keV and hence its intensity cannot be determined. Beyond these previously known transitions, 4 γ transitions with energies higher than 4 MeV were observed. All of them, namely 4596-, 5028-, 5117-, and 5229 keV transitions are in coincidence with the 132-keV ground state transition. The reciprocal coincidences are shown in Figure 7 (c,d) while Figure 7 (e) shows the 132-keV gate where the γ transitions above 5 MeV are shown. The strongest of this set is the 5117-keV for which we could also observe the first and second escape peaks. A gate on the 511 keV annihilation photon in Figure 7 (f) shows the escape peaks for the highest energy γ transitions.

The absolute intensities of all the γ transitions in ^{45}Cl are given in Table II. The level scheme from the current work shown in Figure 6 displays the absolute β feeding branches calculated using the intensities of the γ rays and the total implants obtained from the fit to the decay curve. The branching to the low-lying positive parity states especially to the $1/2_1^+$ and $3/2_2^+$ seems to indicate a significant branch due to FF decay. The SM calculations predict $\log ft$ values of 6.83, 6.95 and 6.84 for the FF transitions to the $1/2_1^+$ and $3/2_{1,2}^+$ states respectively [30] which would be consistent with observed feeding of the $1/2_1^+$ and $3/2_2^+$ states though in the current level scheme the feeding to the ground state is zero. Another source of large feeding to the low lying states has been speculated to be feeding from γ -decay of unbound states as noted in Ref [33]. The states at 4728-, 5160-, 5249-,

and 5361 keV are assumed to be directly fed by GT transitions and the $\log ft$ values are calculated accordingly.

C. ^{45}S ($Z=16$; $N=29$) $\beta 1n$ decay

The large Q_{β^-} value of 14.92(33) MeV for ^{45}S [32] leads to a high β -delayed neutron emission probability (P_n). We followed the γ activity of grand-daughter nuclei in $\beta 0n$, $\beta 1n$ and $\beta 2n$ descendants. The efficiency corrected intensities of the most intense γ transitions in $^{45,44,43}\text{Ar}$ were used to determine the P_n value to be 60(10) % for ^{45}S . The error bar takes into account the correction of growth and decay of activities and the errors in branching ratios. This delayed neutron emission is consistent with β feeding to the bound states of 45(5) % which would be the lower limit as the level could be incomplete due to unobserved γ transitions. The previous measurement of P_n value from Ref. [23] is 54% (errors not quoted in the paper) in agreement with our value. The SM calculations predict a value of 40%, lower than our measured value.

Due to the large β -delayed neutron strength, we were able to observe γ transitions in ^{44}Cl , the $\beta 1n$ daughter. The level scheme proposed by Stroberg *et al.*, [7] from in-beam γ spectroscopy following fragmentation could be verified with the addition of the 481 keV γ decay from the 999-keV state feeding the 518 keV state supported by γ - γ coincidences. Though Ref. [7] did not make any spin-parity assignments to the excited states in ^{44}Cl we proposed them to have negative parity as they are populated via the $\beta 1n$ channel of ^{45}S β decay which has a ground state $J^\pi = 3/2^-$ as tentatively marked in Figure 8. The 891- and 999-keV transitions were also observed in the β -decay of ^{44}S [27] where they would be populated via FF transitions. Specific spin parity assignments will be discussed in the next section.

IV. DISCUSSION

A. $^{43,45}\text{Cl}$: Positive parity states

The ground state of ^{43}Cl is largely assumed to be $1/2^+$ as discussed in the introduction and the first excited state is considered a $3/2^+$ corresponding to the odd proton occupying either the $1s_{1/2}$ or the $0d_{3/2}$ orbital as per the shell model calculations. The shell model

calculations performed for this work further predict a sequence of $1/2^+(gs)$ - $3/2^+$ - $3/2^+$ - $5/2^+$ - $5/2^+$ states for ^{43}Cl (Figure 3). The newly established 879-keV level is thus a candidate for the $3/2_2^+$ state while the 941-keV level is proposed as $5/2_1^+$ consistent with Ref. [5]. We assign the 1669-keV level as the second $5/2^+$ state following the predicted sequence where no assignment was made to this level earlier [7]. The next level at 1836 keV is suggested to have $J^\pi = 7/2^+$. A level at a close by energy of 1830(8) keV was observed in Ref. [5] and proposed as a $7/2^+$ state. The γ transition from that level was 881 keV which could be the 894 keV transition decaying to the $5/2_1^+$ as seen in this work. We also observed the 1507 keV transition from the 1836 keV level to the $3/2_1^+$ state consistent with a $7/2^+$ assignment. The 1927 keV state is a candidate for the $7/2_2^+$ state predicted at a similar energy with a strong decay to the $5/2_2^+$ state.

Shell model predictions for ^{45}Cl are also a sequence of $1/2^+(gs)$ - $3/2^+$ - $3/2^+$ - $5/2^+$ - $5/2^+$ states as the lowest excited states. However in our recent publication [16] following the β^- -decay of ^{45}Cl to ^{45}Ar , we made the argument for a $3/2^+$ ground state of the parent based on the strong population of $5/2^+$ state in ^{45}Ar . Support for a $3/2^+$ ground state for ^{45}Cl was also provided from the earlier observation of strong population of the 4_1^+ state in ^{44}Cl from ^{45}Cl knockout in Ref. [15]. Thus the first five experimental states in ^{45}Cl are proposed as $3/2^+(gs)$ - $1/2^+$ - $3/2^+$ - $5/2^+$ - $5/2^+$ (Figure 6) mostly similar to Ref. [7]. However the state assigned as $5/2_2^+$ in Ref. [7] is incorrect now due to the revised placement of the 1462 keV transition as noted before. The levels at 2391- and 2700 keV are proposed as the $7/2_1^+$ and $7/2_2^+$ states striking a similarity with the observation in ^{43}Cl as also revealed in the calculations. The predicted $7/2^+$ states at 2349 and 2629 would be good counterparts (Figure 6). The 1949 keV level can be a candidate for the predicted 2132 keV, $1/2^+$ state which would be consistent with its decay to the $5/2_1^+$ and $3/2_1^+$ states. In Ref. [7] also they had proposed a $1/2^+$ state above the $5/2_2^+$ state.

B. $^{43,45}\text{Cl}$: Ground state doublet

The ground state spin/parity of odd-A Cl isotopes is determined by the occupancy of the odd proton in either the $1s_{1/2}$ or $0d_{3/2}$ orbital and the lowest transitions of positive parity correspond to the excitation of the proton within the sd shell. In Figure 9 we display the experimentally observed lowest excited states and γ transitions in Cl isotopes from $N = 22$

to $N = 32$ as the neutrons fill up the lower part of the fp shell. Closer to the shell gap at $N = 20$ the ground state is $3/2^+$ with a well separated $1/2^+$ excited state corresponding to a hole in the $1s_{1/2}$ orbital. Away from $N = 20$ the spacing between the $3/2^+$ and $1/2^+$ states is reduced reflective of the near degeneracy of the two orbitals as neutrons fill up the $f_{7/2}$ orbital. Based on experimental observation till now a $1/2^+$ is favored for $^{41,43}\text{Cl}$ whereas a $3/2^+$ assignment is better aligned with various experimental observations. The level structure of ^{45}Cl in the current study further strengthens the proposed $3/2^+$ assignment based on the stronger decay of the $5/2_1^+$ and $5/2_2^+$ states to the $3/2_1^+$ state relative to the $1/2_1^+$ state as was also seen in $^{39,41,43}\text{Cl}$. Predictions of the SM calculations for the decay of these $5/2^+$ states is given in Table III where the trend of strong decays to the $3/2^+$ state can be seen. Consistent results are obtained using both experimental and theoretical energies for the excited states. Thus in ^{45}Cl , with the observation of strong decay of the $5/2^+$ states exclusively to the ground state via the 930- and 1619 keV transitions (no coincidence seen with the 132 keV transition), the assignment of $3/2^+$ to the ground state and $1/2^+$ to the 132 keV state seems more likely.

The odd-A K isotopes show a similar behavior with respect to the lowest $3/2^+$ and $1/2^+$ states. The energy difference between the measured $3/2^+$ and $1/2^+$ states (one of which will be the ground state) is displayed in Figure 10 for isotones of Cl and K with neutron numbers from 20 to 32 (solid symbols connected by thin dashed line). In both cases we start with a $3/2^+$ ground state at $N = 20$ with an inversion at higher neutron number, though for K it happens at a larger neutron excess when the neutrons are filling the $1p_{3/2}$ orbital rather than $0f_{7/2}$ as for Cl isotopes. The energy differences as predicted by the shell model calculations are also shown by the solid lines. The calculations track the experimental observations well as far the inversion of the ground state from $3/2^+$ to $1/2^+$ goes for both, but the return back to a $3/2^+$ ground state is missed at the correct neutron number. Considering that the spin assignments for the ground state for $^{41,43}\text{S}$ are only tentative, a different picture could emerge if future results diverge from the current trends. It should be noted here that the occurrence of a $1/2^+$ ground state in the shell model calculations is a play between the effective single particle energies and deformation.

The occupancies of the first 4 excited states in Cl isotopes obtained from the shell model calculations are plotted in Figure 11. The top panel shows the calculated occupancies for the ground state (solid line) and the first excited state (dashed line) as a function of neutron

number. Δ is the energy difference in keV between the calculated $3/2^+$ and $1/2^+$ states and one can see that the predictions are of a $1/2^+$ ground state (positive Δ) for all isotopes with neutron number from 24 to 30 which is manifested in the occupancy of the $1s_{1/2}$ orbital equal to 1. This differs from the experimental observation where only $N = 24$ and 26 isotopes likely have a $1/2^+$ ground state, though the calculated differences are small. Both the ground state and first excited state have similar occupancies for the fp orbitals with the neutrons shared between $f_{7/2}$ and $p_{3/2}$ similarly.

The bottom panel of Figure 11 shows the occupancies of the excited $5/2_1^+$ (solid line) and $3/2_2^+$ (dashed line) states. The two states again show similar occupation probabilities for the neutrons in the fp orbitals with only differences in how the $\pi s_{1/2}$ and $\pi d_{3/2}$ orbitals are filled. The $3/2^+$ state consistently is formed by one proton in the $1s_{1/2}$ orbital and two in the $0d_{3/2}$ orbital. The $5/2^+$ state on the other hand has a more even distribution for the two orbitals, that is not such a pure configuration. The partial occupancies point towards a more collective nature for the $5/2_1^+$ state, which does follow the energetics of the 2^+ states in the deformed S core as was pointed out in Ref. [19].

C. ^{43,45}Cl: Negative parity states

The negative parity states in the even N (> 20) isotopes of Cl are formed by the promotion of one particle from the sd to the fp shell. According to the shell model calculation based on the $SDPFSDG - MU$ interaction, the dominant configuration of the negative parity states is that of excitation of the unpaired proton from the sd shell to the $0f_{7/2}$ or the $1p_{3/2}$ orbitals accompanied by some rearrangement of the fp shell neutrons.

In ⁴³Cl as shown in Figure 3 the 2022 keV state ($\log ft = 5.88$) is identified as the $3/2_1^-$ state consistent with the predicted state at 2225 keV with a $\log ft$ of 5.87. It has decays to the lower positive parity states via the 2022-, 1692-, 1143, and 1081-keV transition with the ground state transition being the strongest (Table I). The 3032 keV level with decays to the $7/2_2^+$ and $3/2_1^-$ states is proposed to be the $5/2_1^-$ state in agreement with the shell model calculations. Both the 3331- and 3707-keV levels have comparable branches to the $1/2^+(gs)$ and $3/2_2^+$ and are candidates for the shell model states at 3613 keV ($3/2^-$) and 3677 keV ($1/2^-$) and are marked such in the level scheme. The 4249-keV level is proposed to be a $1/2^-$ state as a partner to the shell model state at 4409-keV with a comparable $\log ft$ value.

The levels above that are proposed to have negative parity but conjectures about spin values cannot be made from the current data.

The first 15 negative parity states calculated for $^{43,45}\text{Cl}$ are shown by solid and dashed lines in Figure 12. The solid lines are for spins $1/2^-$, $3/2^-$, $5/2^-$ which will be populated in the β -decay of the odd-A S isotopes, $^{43,45}\text{S}$, while spins of $7/2^-$ and higher are shown as dashed. For both, the solid symbols represent the experimental states that are proposed to have negative parity. In the case of ^{43}Cl we see an excellent agreement between the negative parity states observed here for the first time and the calculated ones. However, as discussed above the spin/parity assignment to the excited states shown in Figure 3 did use guidance from the shell model calculations along with the measured $\log ft$ values and γ branching. The experimental partners to the low spin states not only line up in excitation energy but the $\log ft$ values are consistent too. This highlights the success of the shell model calculations in predicting the structure of both parent and the daughter equally well.

Compared to ^{43}Cl , in ^{45}Cl the negative parity states are predicted higher in energy, with $7/2^-$ as the first negative parity state at 2972 keV (equivalent state in ^{43}Cl is at 2029 keV). The second state in both isotopes is a $3/2^-$; at 2225 keV in ^{43}Cl while at 3678 keV in ^{45}Cl . For ^{43}Cl the experimental state at 2022 keV is in excellent agreement with the predictions with a $\log ft$ value of 5.88, making the $3/2_1^-$ state one of the strongly populated states. Contrary to that, in ^{45}Cl the predicted $3/2_1^-$ state at 3678 keV has a $\log ft$ of 6.61 (Table IV) and we do not have an experimental counterpart to that. Beyond the $3/2_1^-$ state the predicted negative parity states in ^{45}Cl get very close in energy. The experimental states which have been tentatively assigned negative parities all lie above 4.7 MeV and there are counterparts in the shell model calculations (see again Table IV) with spins of $1/2$, $3/2$ or $5/2$ though we cannot make a one to one correspondence for each spin. Compared to ^{43}S decay the $B(GT)$ strength in ^{45}S has moved to higher energies and is a reason for the large β -delayed neutron emission. A plausible explanation for this shift is that with a closed $N = 28$ shell ^{45}Cl may have a spherical configuration in contrast to the parent ^{45}S which is likely to be deformed. States at higher excitation energy thus may provide a better overlap in that case and we may be seeing an influence of deformation in the β -decay strength distribution beyond the more prominent spin selection.

D. ^{44}Cl : Beta-delayed neutron emission

Table IV lists the $\log ft$ values calculated for the allowed GT transitions in the β -decay of ^{45}S (ground state J^π of $3/2^-$) up to 7 MeV whereas the neutron separation energy in ^{45}Cl is 5850(16) keV. We can see that above the neutron separation energy in ^{45}Cl , there are several states with spins $1/2^-$, $3/2^-$ and $5/2^-$ which could be the intermediate states in the β -delayed neutron emission. Neutron emission from these would populate 0^- to 3^- states in the $\beta 1n$ daughter ^{44}Cl if the neutron emitted has an orbital angular momentum $\ell = 0$ which should be the most probable. The partial level scheme of the odd-odd ^{44}Cl from the present study was shown in Figure 8 along with the low lying negative states predicted by the shell model calculations. An odd proton in the $0d_{3/2}$ orbital coupled to an odd neutron in the $0f_{7/2}$ orbital for ^{44}Cl will lead to a multiplet of states with spins from 2^- to 5^- whereas the other possibility of proton in the $0d_{3/2}$ orbital and a neutron in the $1p_{3/2}$ orbital will lead to 0^- to 3^- spin-parity states. These states are very sensitive to the neutron-proton interaction in those orbitals and the low-lying states in ^{44}Cl predicted by the SM calculations do correspond to these configurations (Figure 8).

The first excited state in ^{44}Cl observed at 472 keV is likely a 4^- state based on the $E2$ transition strength deduced from the lifetime estimates in Ref. [34] for the same state. The shell model calculations produce the first 4^- state at 769 keV in reasonable agreement. The 518 keV state is likely a 3^- state in excellent agreement with the shell model state at 489 keV. If the 518 keV state is assigned a 3^- that will limit the spin-parity possibilities for the 999-keV excited state to 1^- , 2^- or 3^- with decay branches to the 3^- state and the 2^- ground state. The states at 726- and 891 keV are candidates for states with $J^\pi = 0^-, 1^-, 2^-, 3^-$ predicted by the shell model calculations with similar energies. The generally good agreement between the states observed in the $\beta 1n$ decay with the predicted low lying spectrum of ^{44}Cl seems to corroborate the conjecture of an $\ell = 0$ neutron being emitted from specific unbound states in ^{45}Cl . Neutron spectroscopy in the future will be greatly helpful in understanding the β -delayed neutron emission process better.

V. SUMMARY

β^- decay of the rare $^{43,45}\text{S}$ isotopes around $N = 28$ shell gap were studied at the NSCL using a 40x40 DSSD as the implant and β detector, surrounded by a γ array of 16 Clover detectors in close geometry. The half-lives were extracted from the fitting of decay curves for $^{43,45}\text{S}$ and are mostly consistent with the earlier work from GANIL. This was the first study of β -delayed γ transitions for these isotopes and led to expanded level schemes for $^{43,45}\text{Cl}$ with negative parity $1p1h$ states identified for the first time. We could provide one more argument in support for a $3/2^+$ ground state for ^{45}Cl while $1/2^+$ for ^{43}Cl .

Large scale shell model calculations using the $SDPFSDG - MU$ interaction provided a good reproduction of the experimental data. The shell model predicts the negative-parity states to be predominantly from proton excitation across the $Z = 20$ shell gap for both $^{43,45}\text{Cl}$. The negative-parity states in ^{45}Cl are found at least an MeV higher than what is seen for ^{43}Cl . On the other hand, if the tentative state in ^{41}Cl at 1475 keV is identified with the SM predicted $7/2_1^-$ (1634 keV) then we also see an upward trend in the occurrence of cross-shell excitations from ^{41}Cl to ^{43}Cl . Also the β^- decay in ^{45}S populates negative parity states higher up in the excitation spectrum. Both of these observations are likely related to moving towards the $N = 28$ shell gap closure for ^{45}Cl .

Following the β -delayed neutron emission, low lying states in ^{44}Cl were also populated which are proposed to be of negative parity. The same states were seen earlier in-beam γ -ray spectroscopy and a few also in the direct β -decay of even-even ^{44}S where they were populated via FF transitions. Tentative spin assignments have been made to these states for now. These states seem to be consistent with an $\ell = 0$ neutron emission from unbound $1/2^-, 3/2^-, 5/2^-$ states in ^{45}Cl .

^{45}S is the heaviest odd-A S isotope, the β^- of which has been studied until now. In our recent publication from this very data set we reported the β^- decay of ^{46}S which is the farthest from stability that can be currently reached for this element. The extension to ^{47}S decay study should be possible with FRIB beams in the near future and will test the predictive powers of shell model calculations in this extremely neutron rich region close to the drip line.

VI. ACKNOWLEDGEMENT

We thank the NSCL operation team and the A1900 team specially Tom Ginter for the production and optimization of the secondary beam. This work was supported by the U.S. National Science Foundation under Grant Nos. PHY-2012522 (FSU), PHY-1848177 (CAREER); US Department of Energy, Office of Science, Office of Nuclear Physics under award Nos. DE-SC0020451 (FRIB), DE-FG02-94ER40848 (UML), DE-AC52-07NA27344 (LLNL), DE-AC02-06CH11357(ANL) and also by the US Department of Energy (DOE) National Nuclear Security Administration Grant No. DOE-DE-NA0003906, the Nuclear Science and Security Consortium under Award No. DE-NA0003180. YU and NS acknowledge KAKENHI grants (20K03981, 17K05433), “Priority Issue on post-K computer” (hp190160, hp180179, hp170230) and “Program for Promoting Researches on the Supercomputer Fugaku” (hp200130, hp210165). SY acknowledges JSPS KAKENHI Grant Number 22K14030 and KAKENHI grant 17K05433 for supporting this work.

-
- [1] C. Force, S. Grévy, L. Gaudefroy, O. Sorlin, L. Cáceres, F. Rotaru, J. Mrazek, N. L. Achouri, J. C. Angélique, F. Azaiez, B. Bastin, R. Borcea, A. Buta, J. M. Daugas, Z. Dlouhy, Z. Dombrádi, F. De Oliveira, F. Negoita, Y. Penionzhkevich, M. G. Saint-Laurent, D. Sohler, M. Stanoiu, I. Stefan, C. Stodel, and F. Nowacki, *Phys. Rev. Lett.* **105**, 102501 (2010).
 - [2] S. Calinescu, L. Cáceres, S. Grévy, O. Sorlin, Z. Dombrádi, M. Stanoiu, R. Astabatyán, C. Borcea, R. Borcea, M. Bowry, W. Catford, E. Clément, S. Franchoo, R. Garcia, R. Gillibert, I. H. Guerin, I. Kuti, S. Lukyanov, A. Lepailleur, V. Maslov, P. Morfouace, J. Mrazek, F. Negoita, M. Niikura, L. Perrot, Z. Podolyák, C. Petrone, Y. Penionzhkevich, T. Roger, F. Rotaru, D. Sohler, I. Stefan, J. C. Thomas, Z. Vajta, and E. Wilson, *Phys. Rev. C* **93**, 044333 (2016).
 - [3] B. Longfellow, D. Weisshaar, A. Gade, B. A. Brown, D. Bazin, K. W. Brown, B. Elman, J. Pereira, D. Rhodes, and M. Spieker, *Phys. Rev. C* **103**, 054309 (2021).
 - [4] M. Mougeot, D. Atanasov, C. Barbieri, K. Blaum, M. Breitenfeld, A. de Roubin, T. Duguet, S. George, F. Herfurth, A. Herlert, J. D. Holt, J. Kartheim, D. Lunney, V. Manea, P. Navrátil, D. Neidherr, M. Rosenbusch, L. Schweikhard, A. Schwenk, V. Somà, A. Welker, F. Wienholtz, R. N. Wolf, and K. Zuber, *Phys. Rev. C* **102**, 014301 (2020).

- [5] O. Sorlin, Z. Dombardi, D. Sohler, F. Azaiez, J. Timar, Y. E. Penionzhkevich, F. Amorini, D. Baiborodin, A. Bauchet, F. Becker, M. Belleguic, C. Borcea, C. Bourgeois, Z. Dlouhy, C. Donzaud, J. Duprat, L. Gaudefroy, D. Guillemaud-Mueller, F. Ibrahim, M. J. Lopez, R. Lucas, S. M. Lukyanov, V. Maslov, J. Mrazek, C. Moore, F. Nowacki, F. Pougheon, M. G. Saint-Laurent, F. Sarazin, J. A. Scarpaci, G. Sletten, M. Stanoiu, C. Stodel, M. Taylor, and C. Theisen, *The European Physical Journal A - Hadrons and Nuclei* **22**, 173 (2004).
- [6] A. Gade, B. A. Brown, D. Bazin, C. M. Campbell, J. A. Church, D. C. Dinca, J. Enders, T. Glasmacher, M. Horoi, Z. Hu, K. W. Kemper, W. F. Mueller, T. Otsuka, L. A. Riley, B. T. Roeder, T. Suzuki, J. R. Terry, K. L. Yurkewicz, and H. Zwahlen, *Phys. Rev. C* **74**, 034322 (2006).
- [7] S. R. Stroberg, A. Gade, T. Baugher, D. Bazin, B. A. Brown, J. M. Cook, T. Glasmacher, G. F. Grinyer, S. McDaniel, A. Ratkiewicz, and D. Weisshaar, *Phys. Rev. C* **86**, 024321 (2012).
- [8] B. D. Linh, A. Corsi, A. Gillibert, A. Obertelli, P. Doornenbal, C. Barbieri, S. Chen, L. X. Chung, T. Duguet, M. Gómez-Ramos, J. D. Holt, A. Moro, P. Navrátil, K. Ogata, N. T. T. Phuc, N. Shimizu, V. Somà, Y. Utsuno, N. L. Achouri, H. Baba, F. Browne, D. Calvet, F. Château, N. Chiga, M. L. Cortés, A. Delbart, J.-M. Gheller, A. Giganon, C. Hilaire, T. Isobe, T. Kobayashi, Y. Kubota, V. Lapoux, H. N. Liu, T. Motobayashi, I. Murray, H. Otsu, V. Panin, N. Paul, W. Rodriguez, H. Sakurai, M. Sasano, D. Steppenbeck, L. Stuhl, Y. L. Sun, Y. Togano, T. Uesaka, K. Wimmer, K. Yoneda, O. Aktas, T. Aumann, F. Flavigny, S. Franchoo, I. Gašparić, R.-B. Gerst, J. Gibelin, K. I. Hahn, N. T. Khai, D. Kim, T. Koiwai, Y. Kondo, P. Koseoglou, J. Lee, C. Lehr, T. Lokotko, M. MacCormick, K. Moschner, T. Nakamura, S. Y. Park, D. Rossi, E. Sahin, D. Sohler, P.-A. Söderström, S. Takeuchi, N. D. Ton, H. Törnqvist, V. Vaquero, V. Wagner, H. Wang, V. Werner, X. Xu, Y. Yamada, D. Yan, Z. Yang, M. Yasuda, and L. Zanetti, *Phys. Rev. C* **104**, 044331 (2021).
- [9] R. Broda, J. Wrzesiński, A. Gadea, N. Mărginean, B. Fornal, L. Corradi, A. M. Stefanini, W. Królas, T. Pawłat, B. Szpak, S. Lunardi, J. J. Valiente-Dobón, D. Mengoni, E. Farnea, M. P. Carpenter, G. De Angelis, F. Della Vedova, E. Fioretto, B. Guiot, R. V. F. Janssens, P. F. Mantica, P. Mason, G. Montagnoli, D. R. Napoli, R. Orlandi, I. Pokrovskiy, G. Pollarolo, E. Sahin, F. Scarlassara, R. Silvestri, S. Szilner, C. A. Ur, M. Trotta, and S. Zhu, *Phys. Rev. C* **82**, 034319 (2010).

- [10] S. Szilner, L. Corradi, F. Haas, G. Pollarolo, L. Angus, S. Beghini, M. Bouhelal, R. Chapman, E. Caurier, S. Courtin, E. Farnea, E. Fioretto, A. Gadea, A. Goasduff, D. Jelavić Malenica, V. Kumar, S. Lunardi, N. Mărginean, D. Mengoni, T. Mijatović, G. Montagnoli, F. Recchia, E. Sahin, M.-D. Salsac, F. Scarlassara, J. F. Smith, N. Soić, A. M. Stefanini, C. A. Ur, and J. J. Valiente-Dobón, *Phys. Rev. C* **87**, 054322 (2013).
- [11] X. Liang, R. Chapman, F. Haas, K.-M. Spohr, P. Bednarczyk, S. Campbell, P. Dagnall, M. Davison, G. de Angelis, G. Duchêne, T. Kröll, S. Lunardi, S. Naguleswaran, and M. Smith, *Phys. Rev. C* **66**, 037301 (2002).
- [12] J. Ollier, R. Chapman, X. Liang, M. Labiche, K.-M. Spohr, M. Davison, G. de Angelis, M. Axiotis, T. Kröll, D. R. Napoli, T. Martinez, D. Bazzacco, E. Farnea, S. Lunardi, and A. G. Smith, *Phys. Rev. C* **67**, 024302 (2003).
- [13] J. A. Winger, H. H. Yousif, W. C. Ma, V. Ravikumar, Y. W. Lui, S. K. Phillips, R. B. Piercey, P. F. Mantica, B. Pritychenko, R. M. Ronningen, and M. Steiner, in *Proc. Conf on Exotic Nuclei and Atomic Masses* (1998).
- [14] J. A. Winger, P. F. Mantica, and R. M. Ronningen, *Phys. Rev. C* **73**, 044318 (2006).
- [15] L. A. Riley, P. Adrich, N. Ahsan, T. R. Baugher, D. Bazin, B. A. Brown, J. M. Cook, P. D. Cottle, C. A. Diget, A. Gade, T. Glasmacher, K. E. Hosier, K. W. Kemper, A. Ratkiewicz, K. P. Siwek, J. A. Tostevin, A. Volya, and D. Weisshaar, *Phys. Rev. C* **86**, 047301 (2012).
- [16] S. Bhattacharya, V. Tripathi, S. L. Tabor, A. Volya, P. C. Bender, C. Benetti, M. P. Carpenter, J. J. Carroll, A. Chester, C. J. Chiara, K. Childers, B. R. Clark, B. P. Crider, J. T. Harke, R. Jain, S. N. Liddick, R. S. Lubna, S. Luitel, B. Longfellow, M. J. Mogannam, T. H. Ogunbeku, J. Perello, A. L. Richard, E. Rubino, S. Saha, O. A. Shehu, R. Unz, Y. Xiao, and Y. Zhu, *Phys. Rev. C* **108**, 024312 (2023).
- [17] M. Ionescu-Bujor, A. Iordachescu, S. M. Lenzi, D. R. Napoli, N. Mărginean, N. H. Medina, D. Bazzacco, D. Bucurescu, G. de Angelis, F. D. Vedova, E. Farnea, A. Gadea, R. Menegazzo, S. Lunardi, C. A. Ur, S. Zilio, T. Otsuka, and Y. Utsuno, *Phys. Rev. C* **80**, 034314 (2009).
- [18] J. W. Olness, A. H. Lumpkin, J. J. Kolata, E. K. Warburton, J. S. Kim, and Y. K. Lee, *Phys. Rev. C* **11**, 110 (1975).
- [19] S. Szilner, L. Corradi, F. Haas, G. Pollarolo, L. Angus, S. Beghini, M. Bouhelal, R. Chapman, E. Caurier, S. Courtin, E. Farnea, E. Fioretto, A. Gadea, A. Goasduff, D. Jelavić Malenica, V. Kumar, S. Lunardi, N. Mărginean, D. Mengoni, T. Mijatović, G. Montagnoli, F. Recchia,

- E. Sahin, M.-D. Salsac, F. Scarlassara, J. F. Smith, N. Soić, A. M. Stefanini, C. A. Ur, and J. J. Valiente-Dobón, *Phys. Rev. C* **87**, 054322 (2013).
- [20] S. Grévy, J. Angélique, P. Baumann, C. Borcea, A. Buta, G. Canchel, W. Catford, S. Courtin, J. Daugas, F. de Oliveira, P. Dessagne, Z. Dlouhy, A. Knipper, K. Kratz, F. Lecolley, J. Lecouey, G. Lehrsenneau, M. Lewitowicz, E. Liénard, S. Lukyanov, F. Maréchal, C. Miehé, J. Mrazek, F. Negoita, N. Orr, D. Pantelica, Y. Penionzhkevich, J. Péter, B. Pfeiffer, S. Pietri, E. Poirier, O. Sorlin, M. Stanoiu, I. Stefan, C. Stodel, and C. Timis, *Physics Letters B* **594**, 252 (2004).
- [21] M. Lewitowicz, Y. E. Penionzhkevich, A. Artukh, A. Kalinin, V. Kamanin, S. Lukyanov, N. Hoai Chau, A. Mueller, D. Guillemaud-Mueller, R. Anne, D. Bazin, C. Détraz, D. Guerreau, M. Saint-Laurent, V. Borrel, J. Jacmart, F. Pougheon, A. Richard, and W. Schmidt-Ott, *Nuclear Physics A* **496**, 477 (1989).
- [22] B. Singh and J. Chen, *Nuclear Data Sheets* **126**, 1 (2015).
- [23] O. Sorlin, D. Guillemaud-Mueller, R. Anne, L. Axelsson, D. Bazin, W. Böhmer, V. Borrel, Y. Jading, H. Keller, K.-L. Kratz, M. Lewitowicz, S. Lukyanov, T. Mehren, A. Mueller, Y. Penionzhkevich, F. Pougheon, M. Saint-Laurent, V. Salamatin, S. Shoedder, and A. Wöhr, *Nuclear Physics A* **583**, 763 (1995), nucleus-Nucleus Collisions.
- [24] Y. Utsuno, T. Otsuka, B. A. Brown, M. Honma, T. Mizusaki, and N. Shimizu, *Phys. Rev. C* **86**, 051301 (2012).
- [25] S. Yoshida, Y. Utsuno, N. Shimizu, and T. Otsuka, *Phys. Rev. C* **97**, 054321 (2018).
- [26] A. Gade and B. Sherrill, *Phys. Scr.* **91**, 053003 (2016).
- [27] V. Tripathi, S. Bhattacharya, E. Rubino, C. Benetti, J. F. Perello, S. L. Tabor, S. N. Liddick, P. C. Bender, M. P. Carpenter, J. J. Carroll, A. Chester, C. J. Chiara, K. Childers, B. R. Clark, B. P. Crider, J. T. Harke, B. Longfellow, R. S. Lubna, S. Luitel, T. H. Ogunbeku, A. L. Richard, S. Saha, N. Shimizu, O. A. Shehu, Y. Utsuno, R. Unz, Y. Xiao, S. Yoshida, and Y. Zhu, *Phys. Rev. C* **106**, 064314 (2022).
- [28] D. Morrissey, B. Sherrill, M. Steiner, A. Stolz, and I. Wiedenhoever, *Nuclear Instruments and Methods in Physics Research Section B: Beam Interactions with Materials and Atoms*, 14th International Conference on Electromagnetic Isotope Separators and Techniques Related to their Applications.

- [29] C. Prokop, S. Liddick, B. Abromeit, A. Chemey, N. Larson, S. Suchyta, and J. Tompkins, Nuclear Instruments and Methods in Physics Research Section A: Accelerators, Spectrometers, Detectors and Associated Equipment **972**, 165432 (2021).
- [30] S. Yoshida, “Betadecaydataprc97.054321,” <https://github.com/SotaYoshida/BetaDecayDataPRC97.054321> (2021).
- [31] NNDC, “<https://www.nndc.bnl.gov/logft/>,” <https://www.nndc.bnl.gov/logft> (2023).
- [32] M. Wang, W. Huang, F. Kondev, G. Audi, and S. Naimi, Chinese Physics C **45**, 030003 (2021).
- [33] A. Gottardo, D. Verney, I. Deloncle, S. Péru, C. Delafosse, S. Rocchia, I. Matea, C. Sotty, C. Andreoiu, C. Costache, M.-C. Delattre, A. Etilé, S. Franchoo, C. Gaulard, J. Guillot, F. Ibrahim, M. Lebois, M. MacCormick, N. Marginean, R. Marginean, M. Martini, C. Mihai, I. Mitu, L. Olivier, C. Portail, L. Qi, B. Roussière, L. Stan, D. Testov, J. Wilson, and D. Yordanov, Physics Letters B **772**, 359 (2017).
- [34] L. A. Riley, P. Adrich, T. R. Baugher, D. Bazin, B. A. Brown, J. M. Cook, P. D. Cottle, C. A. Diget, A. Gade, D. A. Garland, T. Glasmacher, B. A. Hartl, K. E. Hosier, K. W. Kemper, A. Ratkiewicz, K. P. Siwek, D. C. Stoken, J. A. Tostevin, and D. Weisshaar, Phys. Rev. C **79**, 051303 (2009).
- [35] ENSDF, “<https://www.nndc.bnl.gov/ensdf/>,” <https://www.nndc.bnl.gov/ensdf> (2023).

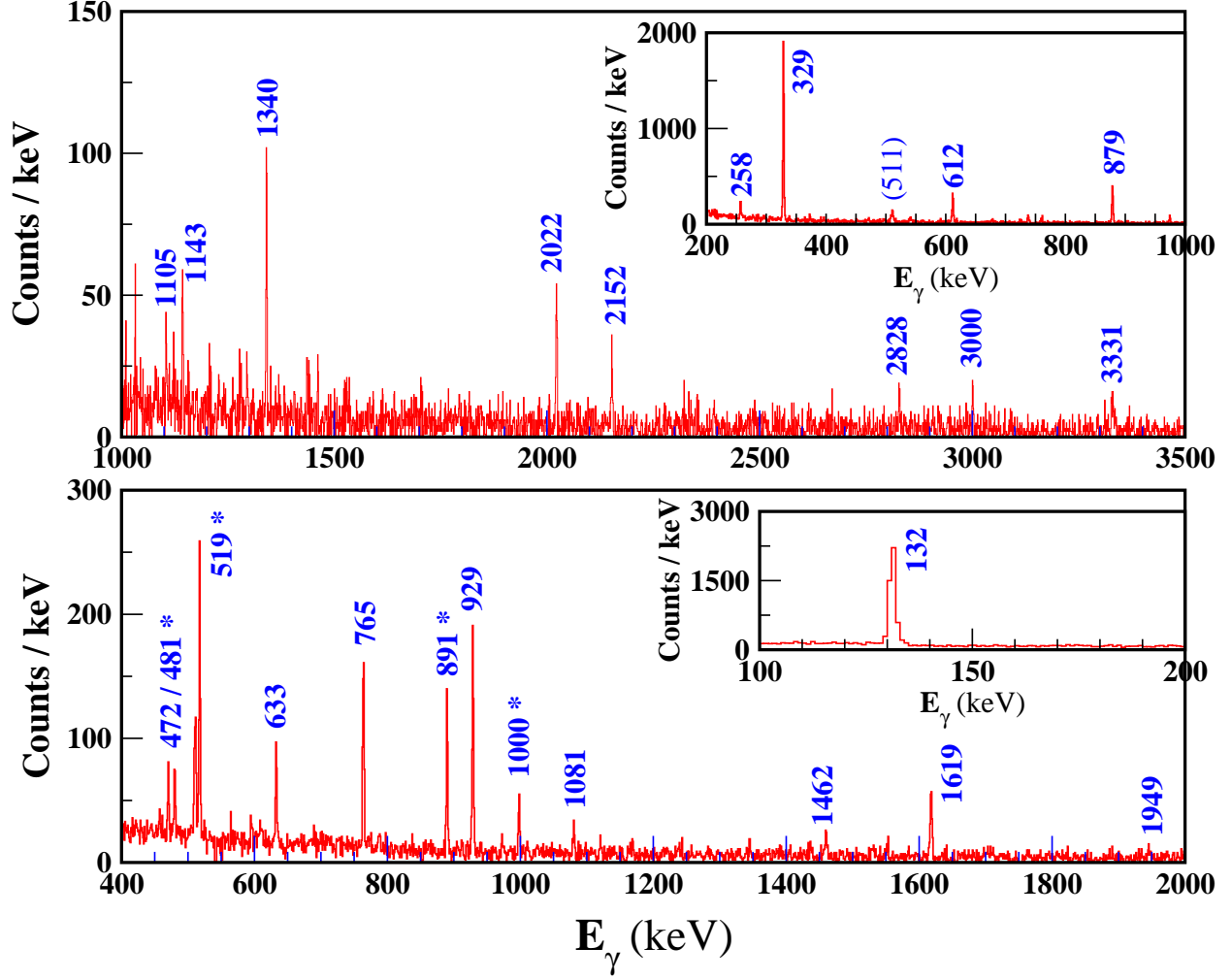


FIG. 1. Top: β -delayed γ transitions in ^{43}Cl for a correlation time window of 200 ms ($\approx 1 T_{1/2}$) after subtracting a background spectrum generated from a 1000 ms correlation window. Bottom: Similarly, β -delayed γ transitions in ^{45}Cl for a correlation window of 100 ms ($\approx 1 T_{1/2}$) after subtracting a background spectrum generated from a 1000 ms correlation window. For both the strong transitions are labeled while the weaker ones are displayed in the coincidence spectra (Figure 4 and Figure 7). Transitions marked with an asterisk in the bottom panel are in the $\beta 1n$ daughter, ^{44}Cl .

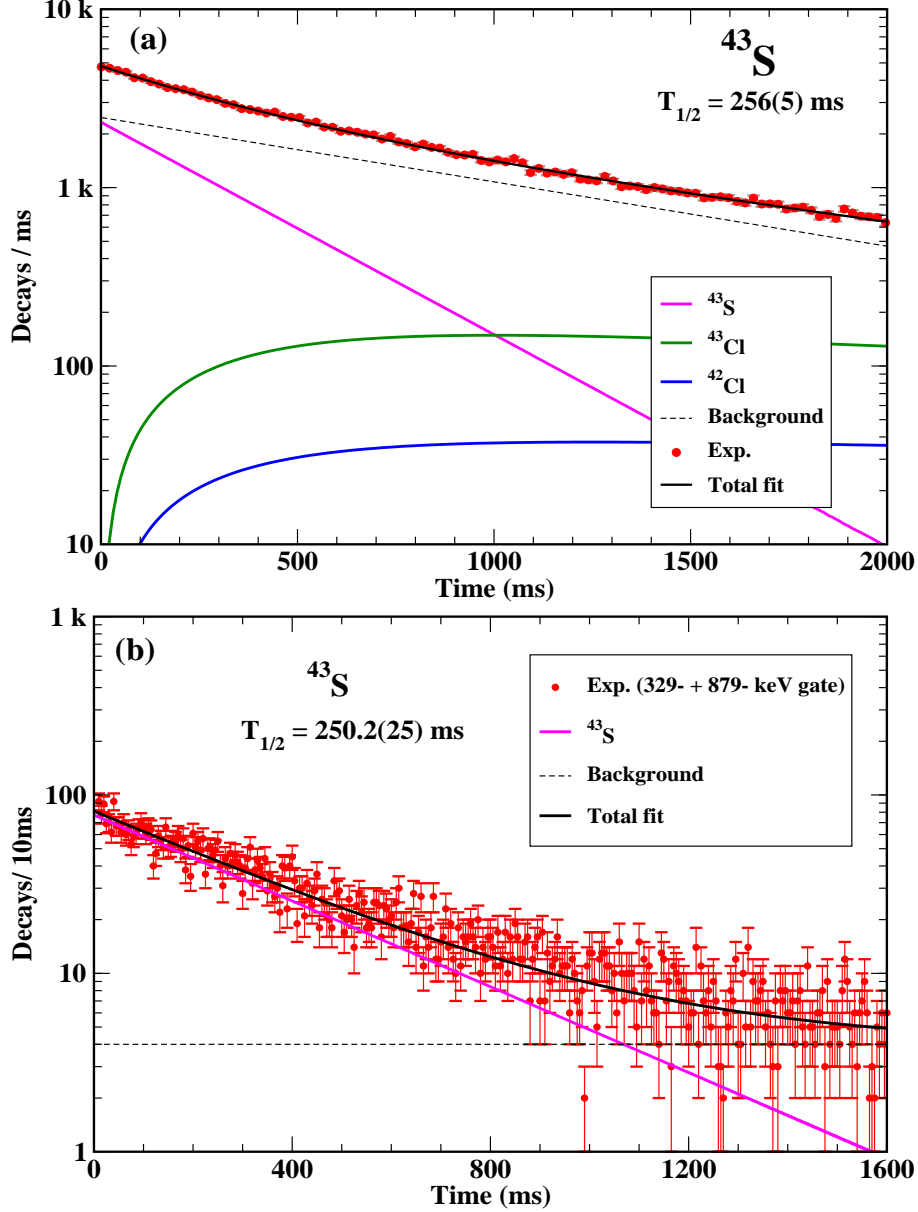


FIG. 2. (a) Decay curve for ^{43}S from β -correlated implants within a grid of 9 pixels in the DSSD for 2 second correlation, along with the fit used to extract half-life and the initial activity. Components of the fit are (i) exponential decay of parent, ^{43}S , (ii) exponential growth and decay of daughter nuclei, ^{43}Cl ($\beta 0n$) and ^{42}Cl ($\beta 1n$), and (iii) exponential background. Known half-lives were used for the daughter nuclides [35]. The half life extracted is 256(5) ms in agreement with the evaluated value, 265(15) ms. (b) Decay curve gated by the 329- and 879-keV transitions the two lowest and strongest transitions in the daughter ^{43}Cl (see Figure 1 and Figure 3). The half life extracted using an exponential fit with a constant background is 250.2(25) ms.

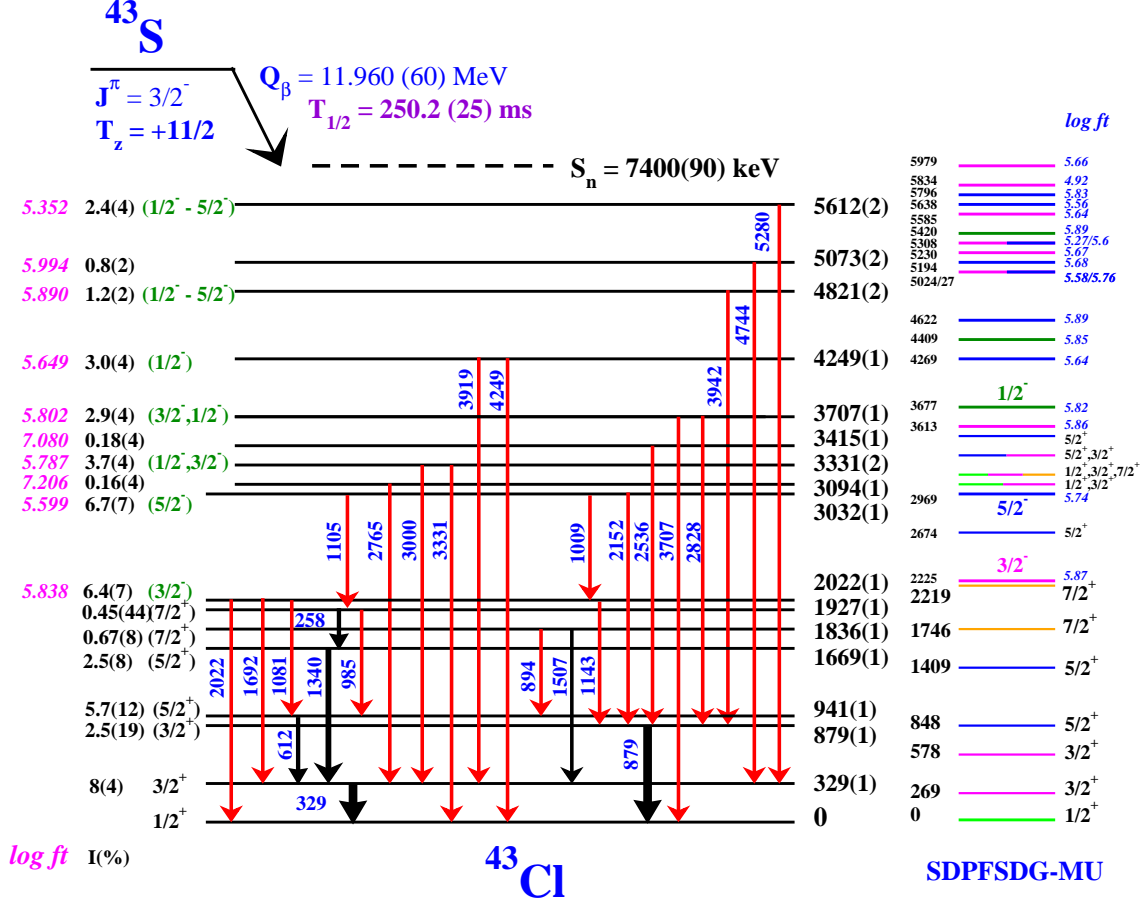


FIG. 3. Partial level scheme of ^{43}Cl following the β^- -decay of ^{43}S ($T_{1/2} = 250.2(25)$ ms and $Q_{\beta^-} = 11.960(60)$ MeV [32]). The transitions marked black were known before this work whereas red indicates the new transitions added in this work. The absolute branching for each level was calculated using the measured yields in the γ transitions feeding in and out of that state, measured γ detection efficiency and total number of implants obtained from the fit to the decay curve. Using the P_n value from Ref. [21, 23] of 40(10)% the feeding to the ground state can be estimated as 13(11)% (not noted in the level scheme as P_n could not be measured for ^{43}S in this work). $\log ft$ values were calculated using the $\log ft$ calculator [31]. Alongside are the predictions of the shell model calculation using the *SDPFSDG-MU* interaction [30]. The positive parity states represent $0p0h$ excitations while the negative parity states are $1p1h$ excitations across the a major shell gap. For protons it will be between *sd* and *pf* shells while neutrons can be excited from the *sd* to the *pf* as well as from *pf* to *sdg* shells. Only selected $1/2^-$ (green), $3/2^-$ (magenta) and $5/2^-$ (blue) states (with $\log ft < 6.00$ and $E^* < 6$ MeV) along with the predicted $\log ft$ values are shown.

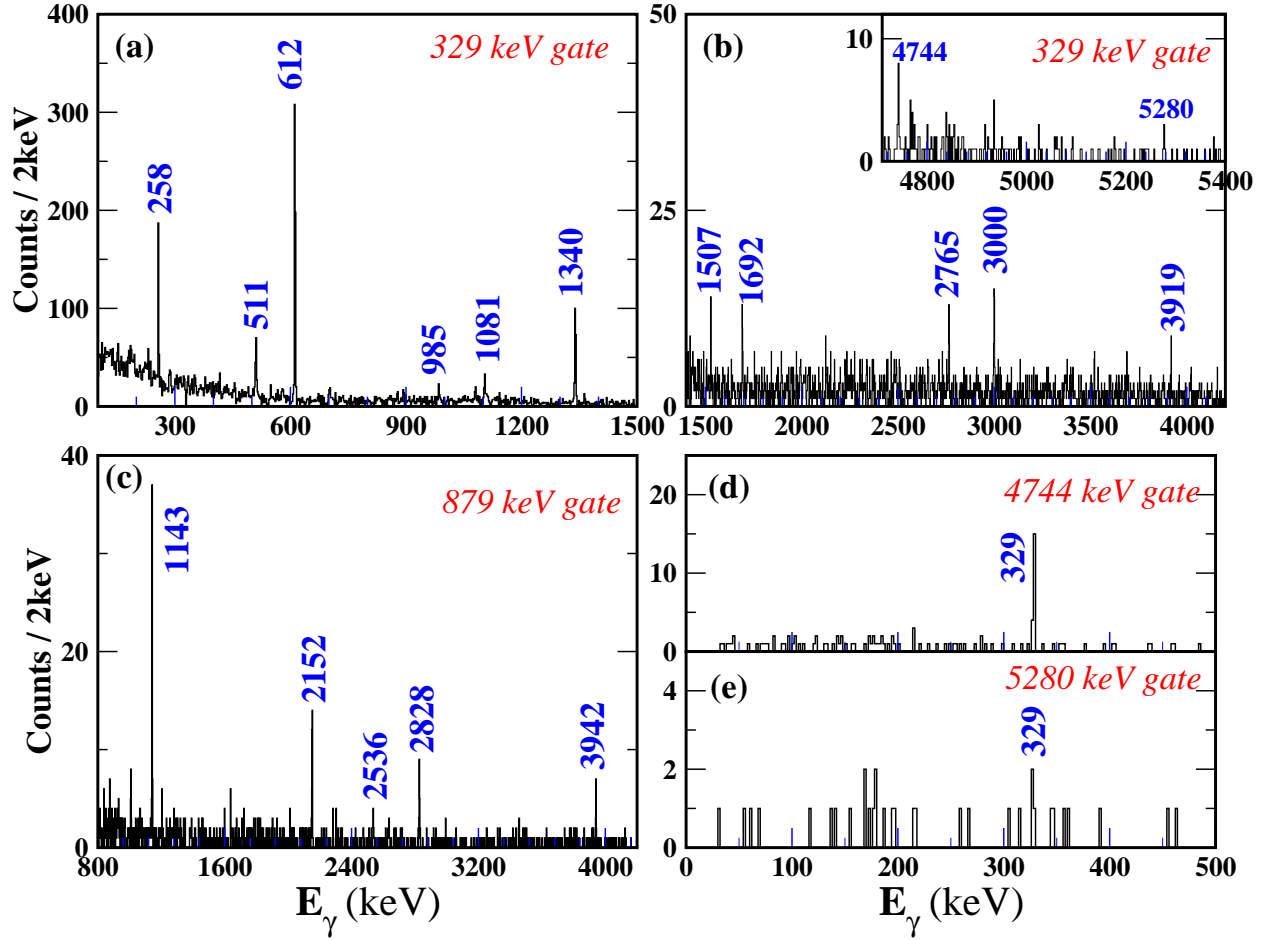


FIG. 4. (a)-(b) γ transitions in ^{43}Cl observed in coincidence with the 329-keV γ transition which de-excites the $3/2_1^+$ state to the ground state. The inset of (b) shows the high energy γ transitions (c) spectrum showing the γ transitions coincident with the 879-keV transition. (d)-(e) the 329-keV transition is seen in coincidence with the high lying 4744- and 5280-keV transitions.

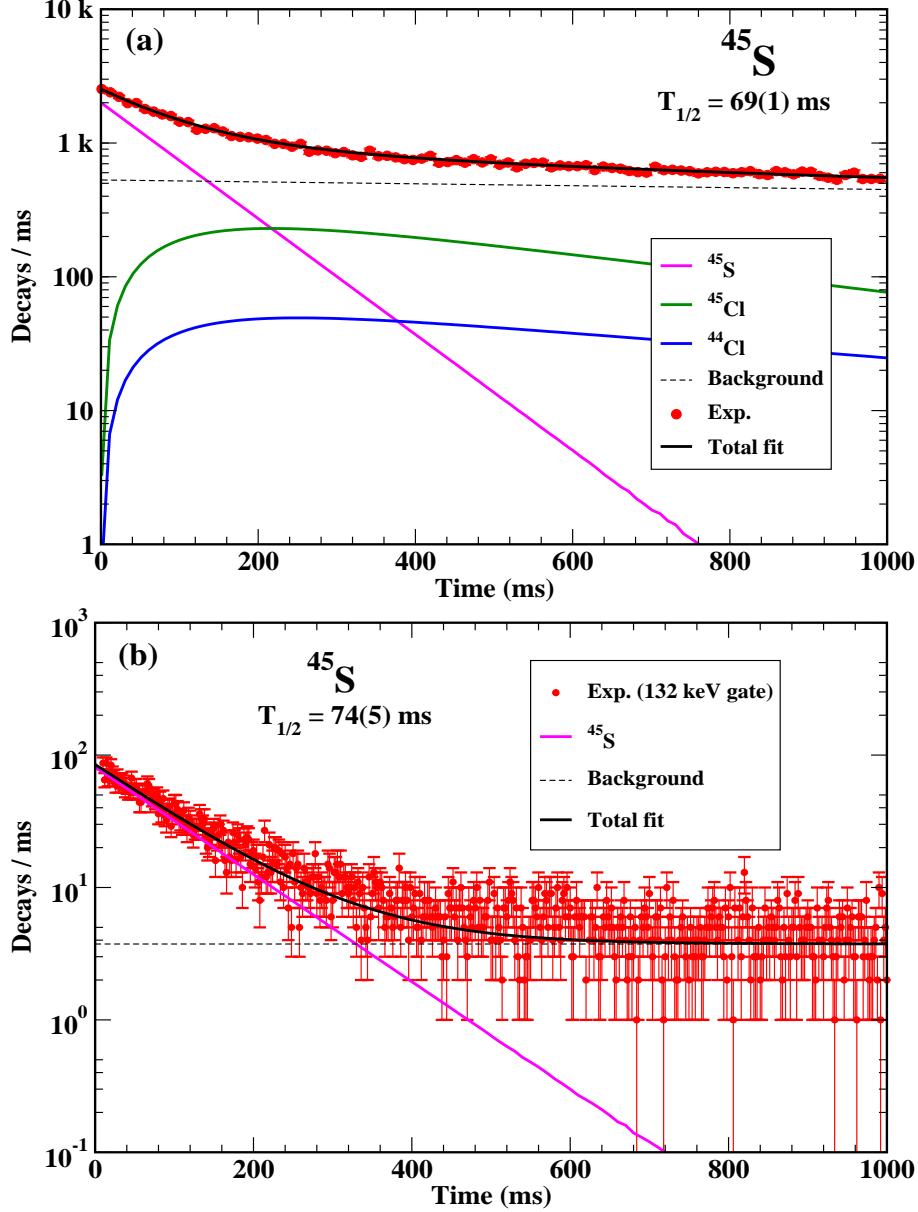


FIG. 5. (a) Decay curve for ^{45}S from β -correlated implants within a grid of 9 pixels in the DSSD, correlated for 1 second along with the fit used to extract half-life and the initial activity. Components of the fit are (i) exponential decay of parent, ^{45}S , (ii) exponential growth and decay of daughter nuclei, ^{45}Cl ($\beta 0n$) and ^{44}Cl ($\beta 1n$), and (iii) background. Known half-lives were used for the daughter nuclides [16, 23, 35]. (b) Decay curve gated by the 132-keV transition which represents the $1/2_1^+ \rightarrow 3/2^+(gs)$ transition in daughter ^{45}Cl . The extracted half-life values are 69(1) ms and 75(5) ms from the two different conditions.

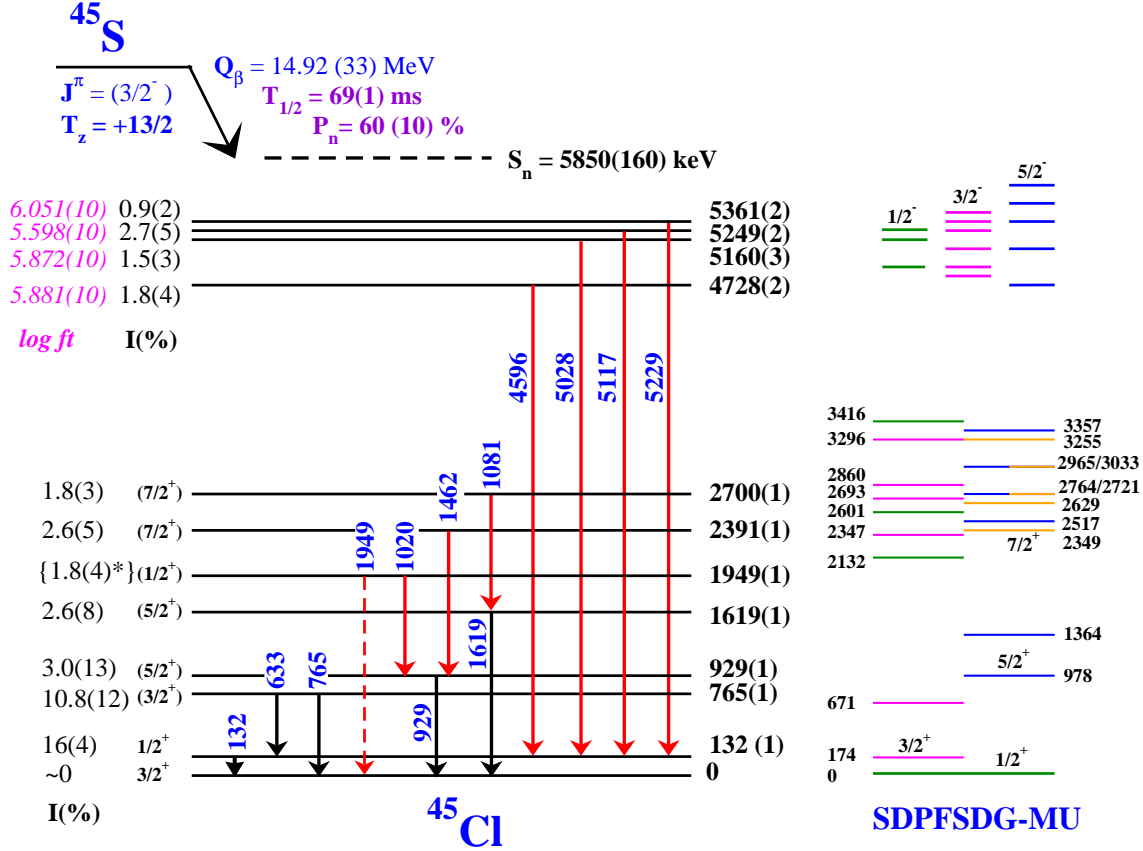


FIG. 6. Partial level scheme of ^{45}Cl following β -decay of ^{45}S ($T_{1/2} = 69(1) \text{ ms}$ and $Q_{\beta^-} = 14.92(33) \text{ MeV}$ [32]). The transitions marked black were known before whereas red indicates the new transitions observed in this study. The absolute branching for each level was calculated similar to that for ^{43}S decay. As the intensity of the 1949 keV transition could not be obtained, the feeding of the 1949-keV level is tentative(*). Based on our measurements the ground state feeding is consistent with zero. SM calculations similar to those for ^{43}Cl are shown alongside. Positive parity states ($0p0h$) with spins of $1/2$, $3/2$, $5/2$ and $7/2$ below 3.5 MeV are shown with different colors identifying the spin values similar to Figure 3. A few representative negative parity states ($1p1h$ excitations in the calculations) are also shown. Only spins $1/2$, $3/2$ and $5/2$ with $\log ft$ values below 6.00 in the energy range of the experimental states (above 3400 keV) are displayed for clarity. The complete list can be seen in Table IV.

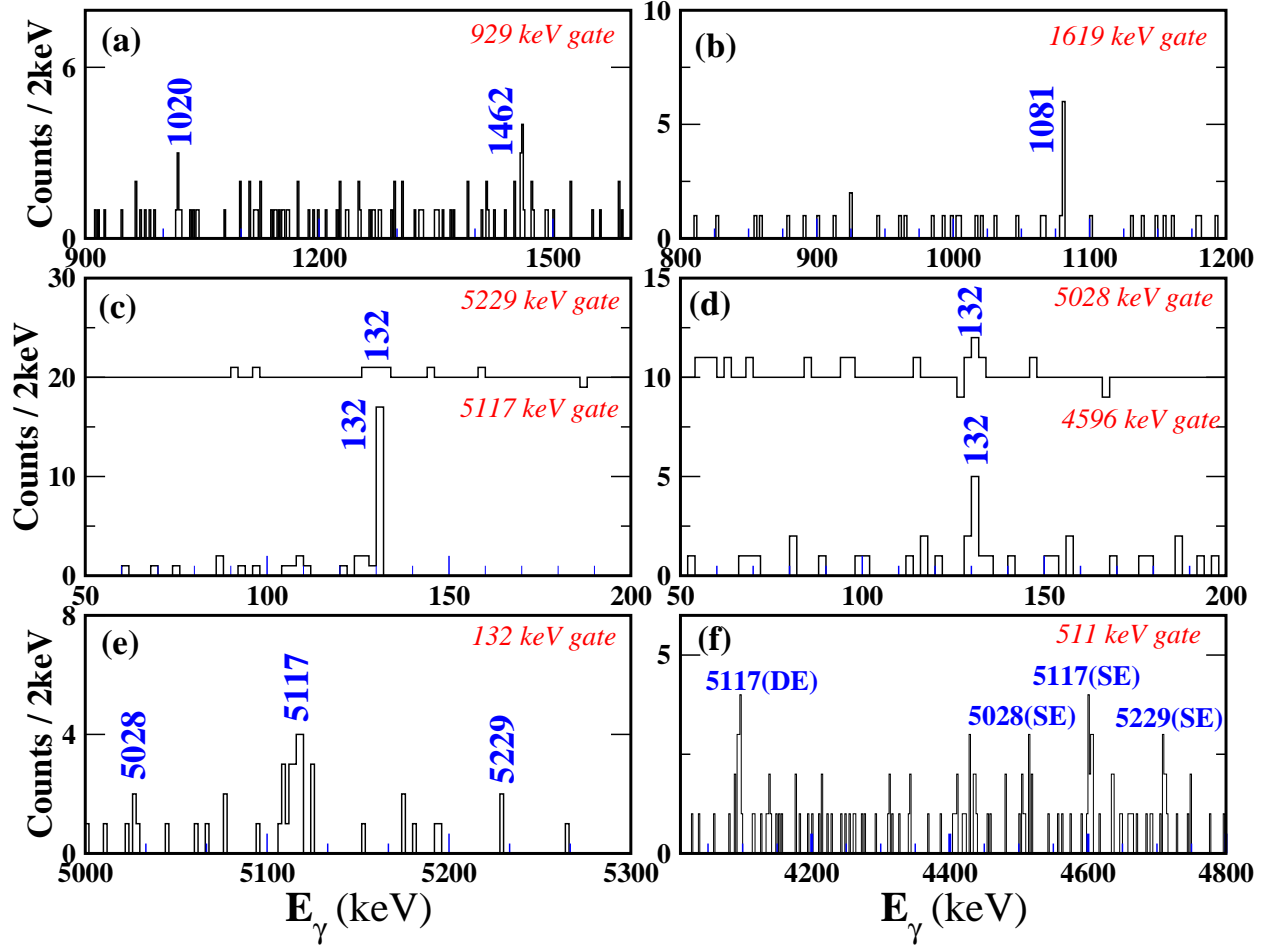


FIG. 7. Spectra displaying the coincidences observed between the γ transitions in ^{45}Cl . (a) the 1020- and 1462- keV transitions are shown in the 929-keV gate. (b) coincidences observed between the 1619-keV and 1081-keV transitions. (c)-(d) The 132-keV transition is seen in the gates of the transitions at 4596-, 5028-, 5118-, and 5229 keV. The y-scales for the 5028- and 5229 keV gates were shifted upwards by 10 and 20 counts respectively for clarity of display. (e) The 5028-, 5118-, and 5229 keV transitions are seen in the 132-keV gate. (f) the gate on the 511 keV γ transition from pair production in the detector which displays the single (SE) and double escape (DE) peaks of the high energy γ transitions as noted.

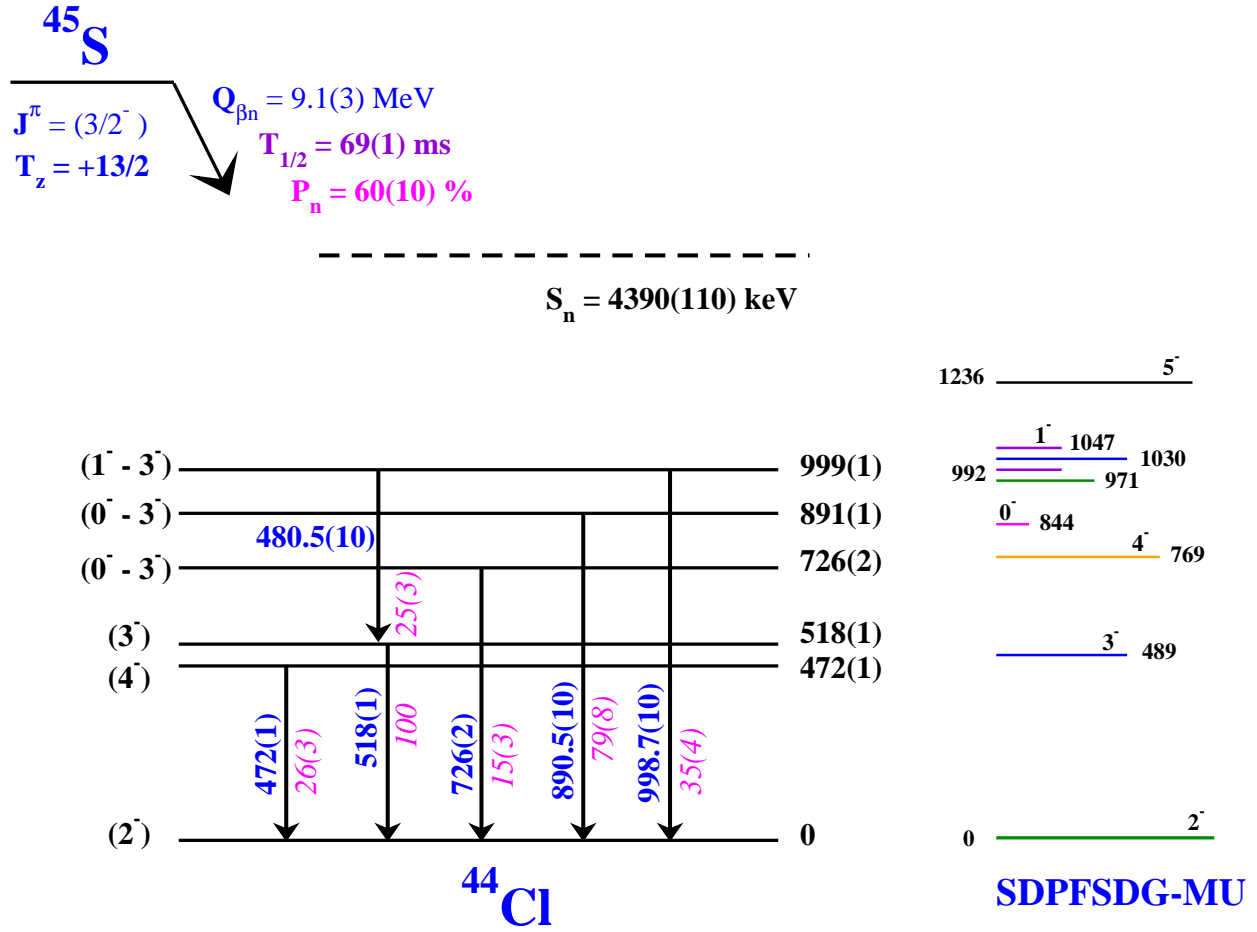


FIG. 8. Partial level scheme of β -delayed neutron daughter ^{44}Cl . The number in italics (magenta) alongside the energy of the transition (in keV) represents the relative intensity with the 518-keV transition taken as 100%. Comparison with SM calculation (shown on the right) and decay pattern have been used to suggest tentative spin-parities of the excited states.

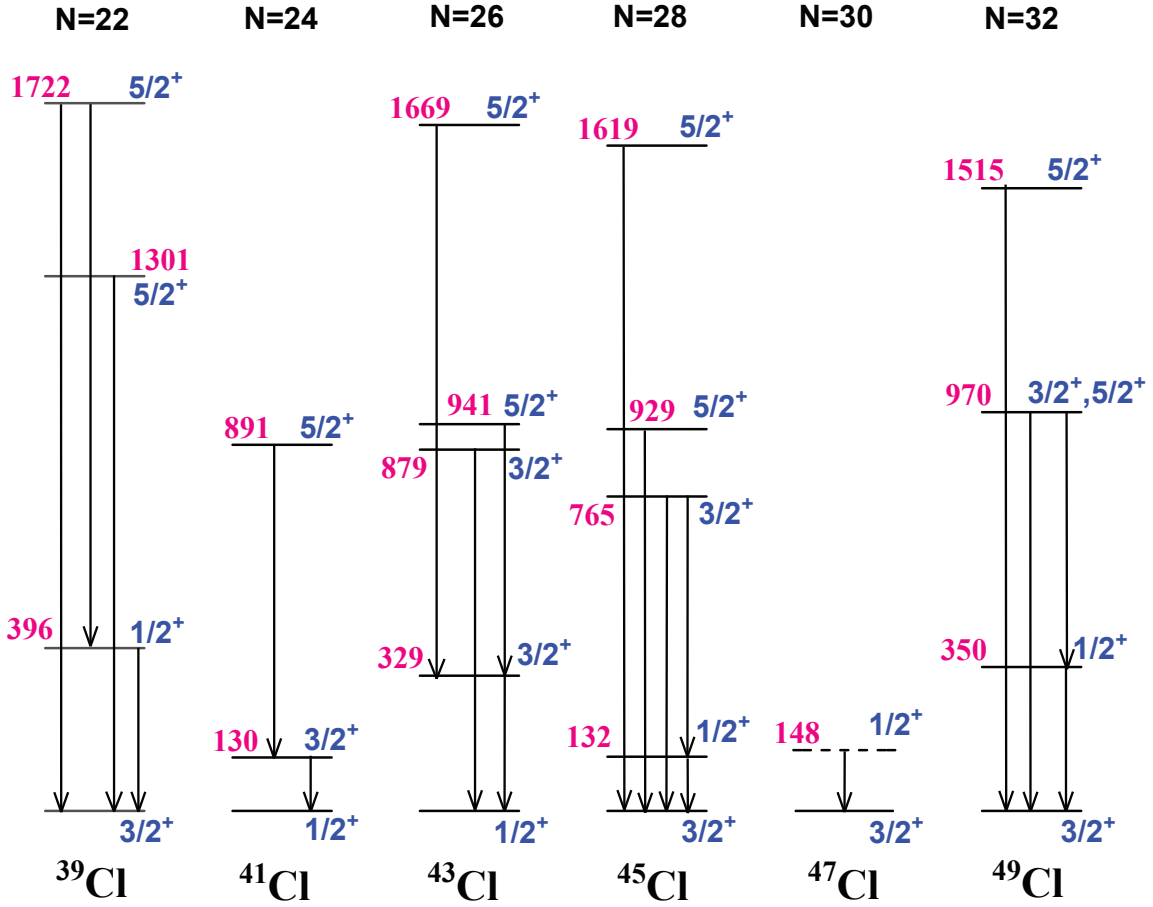


FIG. 9. Comparison of low-lying level structure of odd-A Cl isotopes from $N = 22$ to $N = 32$. The data for $^{43,45}\text{Cl}$ is from the current data set while those of the other isotopes is from published work [35]. Though some of the spin parity assignments are tentative we did not put them in parenthesis for ease of comparison. The point to emphasize here is the strong decay branch for the $5/2^+$ states to the $3/2^+$ state and not to the $1/2^+$ state. The only deviation is for ^{39}Cl where both the branches from the $5/2^+$ state have comparable strength. This is also supported by SM calculations as shown in Table III.

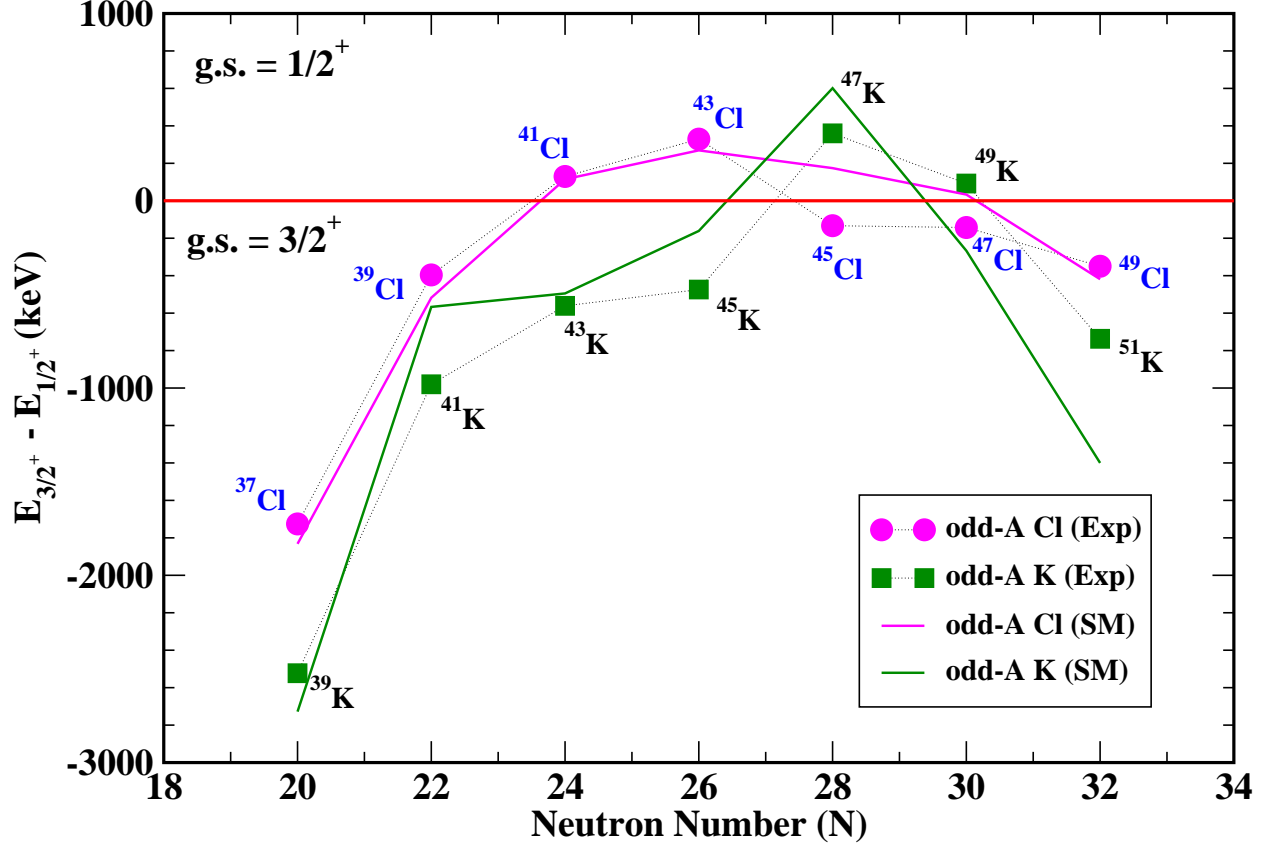


FIG. 10. The energy difference between the first $3/2^+$ and $1/2^+$ states (one of them is the ground state) in odd-A Cl and K isotopes with neutron numbers from 20 to 32 as observed in experiments is shown by the solid symbols connected by thin dashed lines (magenta for Cl and green for K). An inversion of the ground state J^π is seen for both Cl and K for certain neutron numbers. The data for $^{43,45}\text{Cl}$ is from the current data set while those of the other isotopes is from published work [35]. The solid lines are the corresponding energy differences between the $3/2_1^+$ and $1/2_1^+$ states from the SM calculations for the Cl (magenta) and K (green) isotopes.

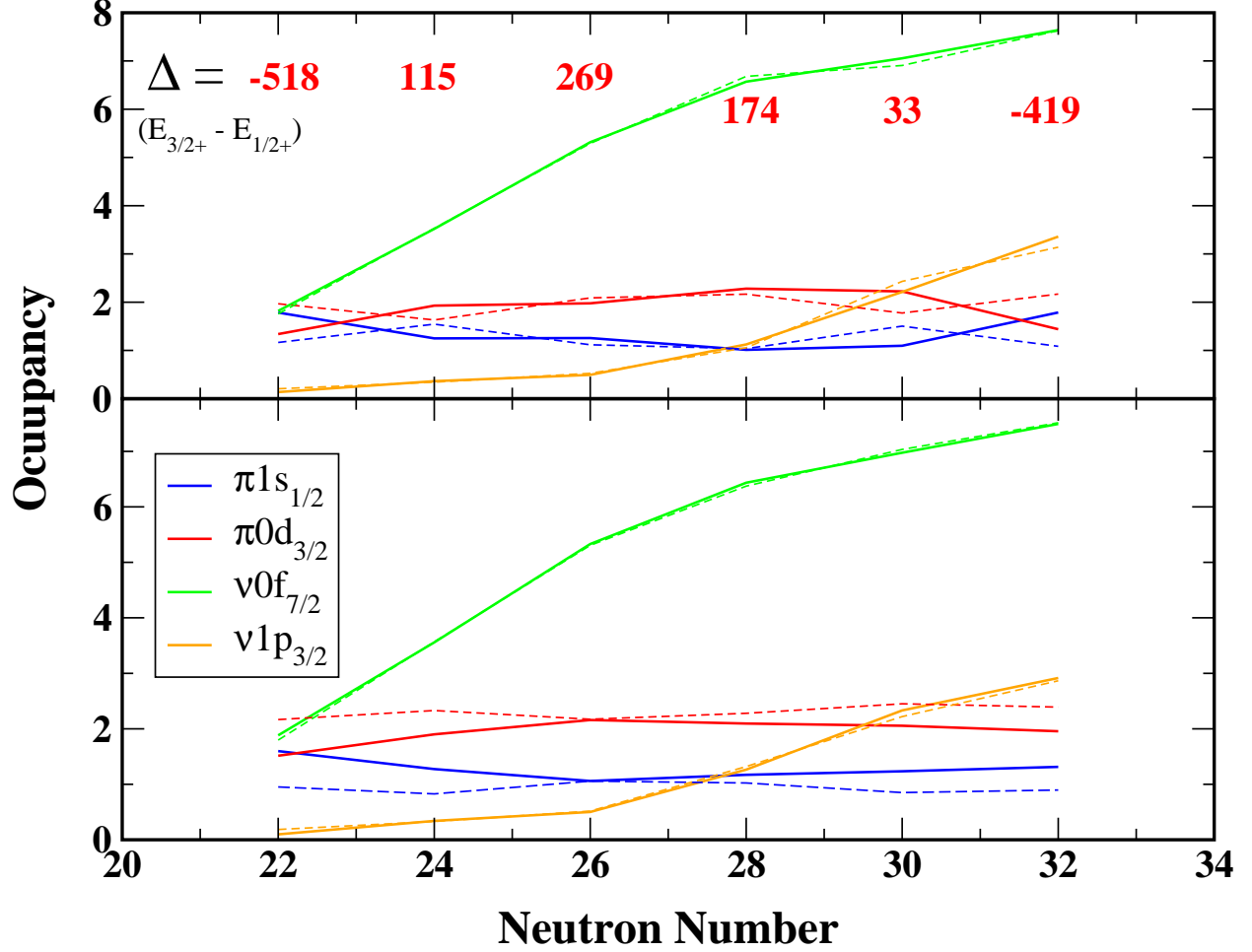


FIG. 11. The predicted occupancies of the proton $s_{1/2}$ and $d_{3/2}$ orbitals and neutron $f_{7/2}$ and $p_{3/2}$ orbitals for the first four excited states in odd-A Cl isotopes are displayed in the top panel. These are orbitals where the valence nucleons would reside in these isotopes. The top panel shows the occupancies for ground state (solid lines) and the first excited state (dashed line). For the ground state and the first excited state, the dominant occupancy of the proton toggles between $0d_{3/2}$ and $1s_{1/2}$ orbitals for these isotopes which leads to the determination of the ground state in the calculations. The energy difference calculated between the $3/2_1^+$ and $1/2_1^+$ (Δ) (in keV) from the shell model calculations is also shown where the negative sign indicates a $3/2^+$ ground state. The bottom panel displays the same for $5/2_1^+$ state (solid line) and $3/2_2^+$ state (dashed line).

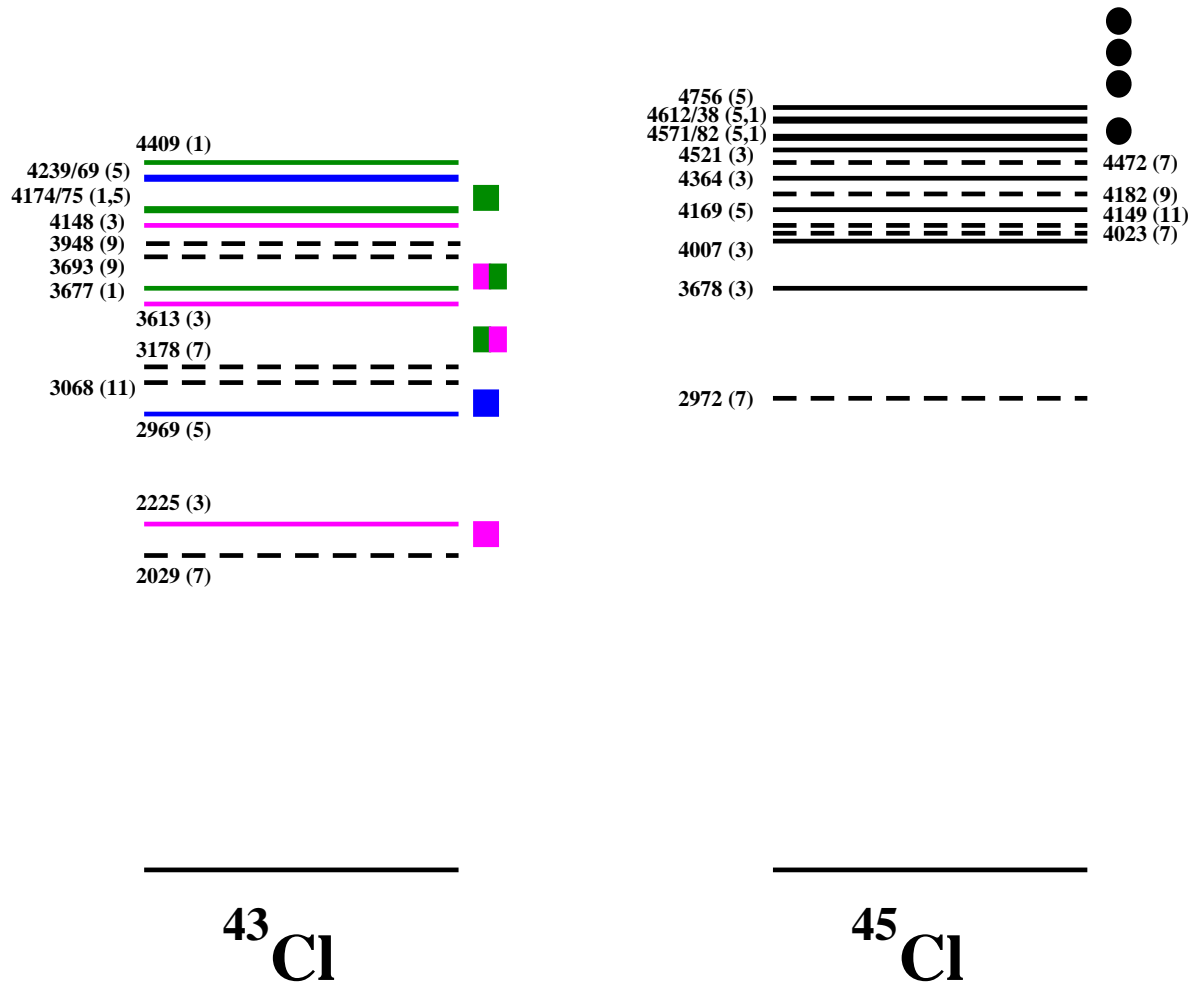


FIG. 12. The first 15 negative-parity states calculated for ^{43}Cl and ^{45}Cl using the *SDPFSDG-MU* interaction are shown. The dashed lines are for spins $7/2^-$ and higher which will not be populated in allowed GT decays while the solid lines show the lower spins. Excitation energy of the states in given in keV and the spin value as $2J$ (in parenthesis) is displayed alongside. The solid symbols represent the experimental states with proposed negative parity in the two cases. For ^{43}Cl the $1/2^-, 3/2^-, 5/2^-$ are matched by colors consistent with what is shown in Figure 3. For ^{45}Cl no spin values have been assigned for the negative parity states and are all shown as black. See text for further discussion.

TABLE I. γ -ray energies, placements and efficiency corrected absolute intensities (per 100 decay events) of transitions in ^{43}Cl from the β decay of ^{43}S decay.

E_γ (keV)	$E_i \rightarrow E_f$ (keV)	I (%)
257.6(5)	1927 \rightarrow 1669	1.97(30)
329.0(4)	329 \rightarrow 0	27.4(41)
612.3(3)	941 \rightarrow 329	7.8(12)
879.1(5)	879 \rightarrow 0	10.9(17)
894.0(10)	1836 \rightarrow 941	0.39(6)
985.0(10)	1927 \rightarrow 941	0.58(9)
1009.4(5)	3032 \rightarrow 2022	0.91(14)
1081.1(5)	2022 \rightarrow 941	1.15(18)
1105.0(5)	3032 \rightarrow 1927	2.1(3)
1143.0(3)	2022 \rightarrow 879	1.96(30)
1340.2(3)	1669 \rightarrow 329	4.5(7)
1506.5(6)	1836 \rightarrow 329	0.28(5)
1692.0(5)	2022 \rightarrow 329	0.49(8)
2022.0(8)	2022 \rightarrow 0	3.67(56)
2152.1(5)	3032 \rightarrow 879	3.7(6)
2536.0(10)	3415 \rightarrow 879	0.18(4)
2765.3(10)	3094 \rightarrow 329	0.16(4)
2828.0(6)	3707 \rightarrow 879	1.4(2)
3000.0(5)	3331 \rightarrow 329	1.6(3)
3331.0(5)	3331 \rightarrow 0	2.1(3)
3707.0(10)	3707 \rightarrow 0	1.5(3)
3919.4(10)	4249 \rightarrow 329	1.4(2)
3942.0(10)	4821 \rightarrow 879	1.2(2)
4249.0(20)	4249 \rightarrow 0	1.6(3)
4744.0(20)	5073 \rightarrow 329	0.8(2)
5280.0(20)	5612 \rightarrow 329	2.4(4)

TABLE II. γ -ray energies, placements and efficiency corrected absolute intensities (per 100 decay events) of transitions in ^{45}Cl from the β decay of ^{45}S decay.

E_γ (keV)	$E_i \rightarrow E_f$ (keV)	I (%)
131.7(5)	132 \rightarrow 0	26(4)
633.3(6)	765 \rightarrow 132	3.3(5)
764.5(5)	765 \rightarrow 0	7.5(11)
929.2(5)	929 \rightarrow 0	7.4(11)
1020.1(10)	1949 \rightarrow 929	1.8(4)
1081.2(10)	2700 \rightarrow 1619	1.8(3)
1461.7(10)	2391 \rightarrow 929	2.6(5)
1618.5(5)	1619 \rightarrow 0	4.4(7)
1949.0(15)	1949 \rightarrow 0	-
4596.0(20)	4728 \rightarrow 132	1.8(4)
5028.4(30)	5160 \rightarrow 132	1.5(3)
5117.1(20)	5249 \rightarrow 132	2.7(5)
5229.0(20)	5361 \rightarrow 132	0.9(2)

TABLE III. Comparison of the calculated decay branches of the first and second $5/2^+$ states to the ground state and the first excited state in $^{39-49}\text{Cl}$ isotopes. As discussed in the text for $^{41,43}\text{Cl}$ the ground state is $1/2^+$ with a $3/2^+$ first excited state and the opposite for other isotopes. The shell model predictions for $B(L)$ values and the experimental excitation (SM calculated excitation) energies were used to calculate the decay rates for the two $5/2^+$ states. In the calculations, the EM transition matrix elements are evaluated with the effective g -factors: $g_\ell^\pi = 1.15$, $g_\ell^\nu = -0.15$ and $g_s = 0.85 * g_s^{bare}$. The effective charges used are $1.35e$ (π) and $0.35e$ (ν). The numbers are quoted for a 100% population of the said state.

Cl isotope	$5/2_1^+ \rightarrow 3/2_1^+$	$5/2_1^+ \rightarrow 1/2_1^+$	$5/2_2^+ \rightarrow 3/2_1^+$	$5/2_2^+ \rightarrow 1/2_1^+$
^{39}Cl	99.7 (100)	0.3 (0)	99.2 (100)	0.8 (0)
^{41}Cl	97.7 (98.4)	2.3 (1.6)	- (100)	- (0)
^{43}Cl	89.6 (92.4)	10.4 (7.6)	98.2 (98.7)	1.8 (1.3)
^{45}Cl	97.2 (88.7)	2.8 (11.3)	98.1 (96.9)	1.9 (3.1)
^{47}Cl	- (64.4)	- (35.6)	- (98)	- (2)
^{49}Cl	95.3 (93.8)	4.7 (6.2)	56.5 (59)	43.5 (43)

TABLE IV. Shell model predictions for the β^- decay of ^{45}S with a ground state $J^\pi = 3/2^-$. Excited states up to 7 MeV in ^{45}Cl with spins of $1/2^-$, $3/2^-$, and $5/2^-$ expected to be populated in allowed GT decay are given with the calculated $\log ft$ values.

$3/2^- \rightarrow 1/2^-$		$3/2^- \rightarrow 3/2^-$		$3/2^- \rightarrow 5/2^-$	
E_{level} (keV)	$\log ft$	E_{level} (keV)	$\log ft$	E_{level} (keV)	$\log ft$
4583	8.26	3678	6.61	4.170	6.97
4369	7.19	4008	6.83	4572	6.18
4956	5.67	4365	6.73	4612	7.76
5209	6.88	4522	6.17	4757	5.93
5253	5.70	4873	5.48	4959	7.07
5396	6.13	4968	5.53	5022	6.28
5567	9.20	5161	5.48	5187	5.40
5746	7.90	5301	5.72	5377	5.55
6003	6.43	5396	5.33	5515	5.76
6089	6.44	5501	5.31	5712	5.38
6355	6.38	5670	5.75	5900	4.97
6483	6.22	5928	5.43	5991	5.37
6699	6.03	6074	5.65	6281	5.53
6997	5.98	6382	5.90	6532	5.37
		6723	6.14	6797	5.30
		6992	5.66	7029	5.35